Statistical Analysis of Asian Weather Derivatives

A Master Thesis presented

by

Yue Jiao

(521756)

to

Prof. Dr. Wolfgang Härdle

Institute for Statistics and Econometrics
CASE - Center for Applied Statistics and Economics

Humboldt-Universität zu Berlin

in partial fulfillment of the requirements
for the degree of

Master of Economics and Management Science

Berlin, 15.September, 2009

Abstract

Since last decade, weather derivatives have been traded by Chicago Mercantile Exchange(CME) to hedge the weather risk. In addition to HDD,CDD and CAT, which are index written on the temperature in U.S. and Europe, Pacific Rim Index is newly developed and actively traded nowadays. In terms of the great value of research on this new instrument, we study the temperature dynamics of 4 cities in Asia: Tokyo, Osaka, Taipei and Beijing by a continuous-time autoregressive process. We further inferred the market price of risk from Tokyo and Osaka futures on CME as both a piecewise constant linear function and a time-dependent object. At last, we estimated Tokyo & Osaka future prices with the extracted market price of risk, and studied the risk premium with respect to the prices when market price of risk equals to zero.

Key Words: Weather derivatives, Continuous-time Autoregressive model, Pacific Rim Index, Market Price of Risk

Contents

List of Figures

List of Tables

1 Introduction

Weather has been influencing our individual's life as well as industrial revenue. A survey of PricecooperWaterhause as presentation to Weather Risk Management Association in 2005 has released the top 5 industries that are facing with weather risk, they are energy, agriculture, retail, construction and transportation.Weather risk is about the unpredictable component of weather fluctuation-"weather surprises", or "weather noise".To assess the potential for hedging against weather surprises, and to formulate the appropriate hedging strategies, one needs to determine how much weather noise exists that can be eliminated by weather derivatives.(Campbell&Diebold 2005)

Weather derivative starts to be traded in the latest decade, with the form of weather options, weather swaps, etc, whose payoff are written on varies underlying weather events, such as cooling degree day, heating degree day, average temperature, precipitation, sunshine etc. Chicago Mercantile Exchange have been trading weather derivatives since 1999, and developed into the world's biggest organized market of weather derivatives with future, option, seasonal strips and swap of weather events all around world.

The market of weather derivatives in Asia is newly developed but prosperously growing and attracting more and more investors.Temperature of two Asia-Pacific cities': Tokyo and Osaka are being traded on Chicago Mercantile Exchange. Starting from 2000, the trading volume of these two cities' temperature derivatives have been growing with a rate of 10% per year(PwC 2005),driving the growth of the whole CME weather derivatives trading all around the world. In terms of the influence and potential of this new market, the studies on asian weather derivative is of great value of research.

With the booming of the trading market of weather derivative, various practices regarding this new and interesting financial instruments have also emerged. The pilot result came from Dornier & Querel (2000), in which constant variance of the temperature observations at Chicago O'Hare airport was taken to fit the Ornstein-Uhlenbeck stochastic process. The same model was extended by Alaton et al.2002,

which applied a monthly variation in the variance of temperature observations of Bromma airport outside Stockholm. Campbell et al.2005 applied 4 US cities temperature into a higher-order autoregressive model and investigated the seasonality in the autocorrelation function for the squared residuals. Mraoua et al. 2005 studied the data from Casablanca, Morocco, by a mean reverting model with stochastic volatility, based on which a temperature swap was priced.

Concerning pricing techniques, various studies have been proposing different approaches, trying to answer the question of choosing the right price among a continuum of possible arbitrage-free prices.Davis et al. 2001 proposed to use a marginal utility technique to price temperature derivatives based on the HDD-index. Barrieu et al. 2002 challenged the reasonability of the standard risk neutral point of view in valuating weather derivatives in terms of their iliquidity, and further presented an optimal design of them. Cao et al. 2004 and Richards et al.2004 extended Lucas' equilibrium pricing model to avoid the direct estimation of market price of weather risk, then price the weather derivative on the base of the stochastic processes of the weather index, an aggregated dividend and an assumption about the utility function of a representative investor. Platen et al. 2005 suggested a new numeraire to price temperature derivatives as world stock index. Benth et al.2005 and 2007 proposed the continuous time autoregressive model with seasonality for the temperature evolution in time and match this model to data observed in Stockholm, Sweden. They derived future and option prices for contracts on CDD and CAT indices. They also discuss hedging strategies for the options and the volatility term structure. Hamisultane et al.2007 carried out an empirical study for the New York over the counter (OTC) future prices extract the risk neutral distribution and the market price of weather risk. Horst et al. 2007 solved an individual agents optimization problem under the assumption that the risk bond completes the illiquid financial market and they characterized the equilibrium market price of risk in terms of a solution to a nonlinear PDEs. Hung-Hsi et al. 2008 extended the long term temperature model proposed by Alaton et al. 2002 by taking into account ARCH/GARCH effects to remove the clustering of volatility temperature. They examine the effects of mean, variance and market price of risk on HDD/CDD option prices and demonstrate that their effects are similar to those on the prices of traditional options.

Benth et al. 2007 has launched a pilot studies on the weather derivatives. In

order to study the dynamics of the temperature, a higher order continuous time autoregressive model was proposed. They firstly decomposed the temperature with a seasonality function and an autoregressive process, in which they assumed that the volatility follows a seasonal variance and the residual is a white noise. By applying the temperature of Stockholm, Sweden, into this proposed model, Benth et al.2007 detected clear seasonal variations in the autoregressive residuals, thus justified the reliability of the proposed model. After achieving Gaussian residuals, they proceed with a continuous time autoregressive process with the parameters coming from the previous autoregressive model. Further, they derived an explicit form for future prices of Heating Degree Day (HDD), Cooling Degree Day (CDD) and Cumulative Average Temperature (CAT) with the methods in financial mathematics. At last, the prices of options and their associated hedging strategies were analyzed.

With the justified soundness of the stochastic model from Benth et al.2007,, Härdle et al. 2009 fit the temperature data observed in Berlin to the suggested temperature model and further extend the studies of pricing weather derivatives with a new parameterization method: Market price of risk(MPR). MPR was firstly introduced in Brigo et al.2001 for interest rate theory. It is a new parameter that can be calibrated to data, then use the market to pin down the price. As weather is a non-tradable asset, MPR is of great necessity to be applied as a pricing approach in this scenario, and it also adjusts the underlying process so that the level of the risk aversion is not needed in evaluation. Härdle et al. 2009 studied the MPR of weather in Berlin not only as a piecewise constant linear function, but also a as time dependent object. With the estimated MPR from Berlin Cumulative Average Temperature (CAT), they priced the new derivatives e.g. Cooling Degree Day (CDD) and Heating Degree Day (HDD). They also suggested the application of the MPR estimate into the hedging and pricing of the non-standard maturity contracts and the other over the counter(OTC) market.

Our studies on Asian Weather Derivatives will be based on the methods of stochastic modeling of the temperature data, suggested by Benth et al. 2007 and the methods of pricing with MPR, from Härdle et al. 2009. Empirically, in modeling the temperature data, we observed not only a seasonal volatility in the residuals of autoregressive model, but also a clustering of volatility, thus an additional step using generalized autoregressive conditional heteroscedasticity (GARCH) was applied in

order to achieve the Gaussian residuals. Campbell et al.2005 has provided us with justified soundness of this application by evidence from the modeling of 4 American cities. The residuals afterwards appear to closer to normality, compared with the result from not applying GARCH model.

Our paper also contributes by another extension of applying Local Linear Regression to simplify the volatility modeling. After we achieved the normality of residuals with a "2-Step Approach" including a truncated Fourier series, suggested by Benth et al. 2007 and GARCH model, presented by Campbell et al. 2005, we tried to shorten the procedure by applying a "1-Step Approach" - Local linear Regression with Epanichnikov Kernel. This 1 step modeling has effectively captured the seasonal and cyclical volatility; the residuals afterwards are even closer to normality compared with the "2-Step Approach". Asian weather derivative, Pacific Rim Index, as a new index traded in Chicago Mercantile Exchange, has not been analyzed in any previous studies. Thus we aim to propose a pilot studies in this field, not only precisely model the temperature in Asia, but also present a sound model in pricing Pacific Rim Index in Asia.

The paper is structured as following: in the second section, we introduce the market of weather derivative in Asia and define the product that we are going to analyze. In section 3, we analyze the temperature data in Asia by econometric methods, with both a "2-Step Approach" and "1-Step Approach". In section 4, we shall explain the connection of the weather dynamics and the pricing methodology, and then derive a pricing model for future price, with which we imply the MPR from the index on CME and estimated the prices with different parametrization methods for a comparison aiming to measure the risk premium with respect to zero MPR. Section 6 is the conclusion. All of the computation was done by Matlab version R2008b. The data set of temperature as well as weather derivative was provided by Bloomberg professional service.

2 Market for Temperature Derivatives

In this section, we are going to introduce the temperature index traded on Chicago Mercantile Exchange(CME), especially the index regarding Asian weather in details.

2.1 Temperature Derivative Worldwide

Since 1999, Chicago Mercantile Exchange has been launching varies temperature derivatives in order to protect the enterprisers against the weather related risk. 10 years of endeavoring has resulted in a tremendous growth worldwide. Nowadays, 4 main temperature products are being traded on CME, covering 18 U.S, 9 European and 2 Aisa-Pasific cities.

A glance over the Table 1.1 would show us the variety of contracts being traded in CME as well as their specific properties. Weather contracts for the winter months in U.S. and European cities are classified according to an index of Heating Degree Day (HDD) values, days in which energy is used for heating. The contracts for U.S. cities in the summer months are geared to an index of Cooling Degree Day (CDD) values, days in which energy is used for air conditioning. In Europe, CME Weather contracts for the summer months are based on an index of Cumulative Average Temperature (CAT). In Asia, CME Weather contracts for the whole year around is based on the Pacific Rim Index. Jewson et al.(2005)

	U.S.	Europe	Asia-Pacific
Contract Type	HDD& CDD	HDD&CAT	Pacific Rim Index
Contract Size	20$	20£	2,500¥
Degree Measure	^oF	^oC	^oC
Contracts Month	Heating Season (11-5) Cooling Season (5-9)	Heating Season (11-5) Cooling Season (5-9)	All Year Around

Table 1.1: CME Weather Contracts Specifications

Several common properties of contracts traded in U.S. market and Europe market can be summarized as follows:

Firstly, the minimum fluctuation of the contract value is 1 degree day index for all of the index traded on CME.

Secondly, the maximum value of the contract is 10,000 local currency times the tick size of the contract.

Thirdly, the contract size is 20 local currency, namely U.S. dollars and Britain Pounds, times the degree day index.

Fourthly, contracts traded in U.S. and Europe follows a 2-season rule, by which the whole year is divided into cooling season and heating season. Contracts are issued and settled within the season.

A detailed description of different contracts are found in the following paragraphs.

2.1.1 HDD

Heating Degree Day(HDD)measures the accumulation of the degree days(daily average temperature) which is above a specific baseline (usually 18^oC or 65^oF).The HDD index measures the temperature over a period $(\tau_1, \tau_2)$and is defined as:

$$HDD(\tau_1, \tau_2) = \int_{\tau_1}^{\tau_2} \max(18^oC - T_t, 0)dt \tag{1}$$

An HDD value represents the number of degrees the day¡¯s average temperature is lower than 18^oC. For example, an average daily temperature of 15^oC would generate a daily HDD value of 3^oC (18-15=3).If the temperature exceeds 18^oC, the value of the HDD would be zero, as theoretically, there won't be heating.

2.1.2 CDD

Cooling Degree Day(CDD), on the other hand, measures the accumulation of the degree days(daily average temperature) which is below a specific baseline (usually 18^oC or 65^oF).The CDD index measures the temperature over a period $(\tau_1, \tau_2)$and is defined as:

$$CDD(\tau_1, \tau_2) = \int_{\tau_1}^{\tau_2} \max(T_t - 18^oC, 0)dt \tag{2}$$

An HDD value represents the number of degrees the day¡¯s average temperature is higher than 18^oC. For example, an average daily temperature of 25^oC would generate a daily CDD value of 7^oC (25-18=7).If the temperature is lower than 18^oC, the value of the CDD would be zero.

Monthly HDD or CDD index values are simply the sum of each daily HDD or CDD value recorded during a given month or season. For example, if there were 10 HDD daily values recorded in November 2008 in Berlin, the November 2008 HDD index would be the sum of the 10 daily values.

Thus, if the HDD values were 25, 15, 20, 25, 18, 22, 20, 19, 21 and 23 the monthly HDD index value would be 208. The value of a CME Weather futures contract is determined by multiplying the monthly HDD or CDD value by £20. Using the example above, the CME November Weather contract would settle at £4160 (£20 x 208 = £4160).

2.1.3 CAT

Cumulative Average Temperature(CAT)is the index traded regarding the temperature in Europe. It measures accumulation of daily average temperature within period(τ_1, τ_2) and is defined as:

$$CAT(\tau_1, \tau_2) = \int_{\tau_1}^{\tau_2} T(t)dt \tag{3}$$

2.2 Temperature Derivative in Asia

While HDD,CDD and CAT written on temperature in U.S. and Europe are widely traded, CME has launched new products regarding 2 Japanese cities: Tokyo and Osaka.

2.2.1 Pacific Rim Index

Pacific Rim Index shows a similar characteristic as cumulative average temperature by accumulating the daily average temperature in the whole month of measurement period. Shown in Table 1.2, we see that there is no big deviation from the index price on CME and the accumulated monthly temperature in the real world, which justifies the similarity between the Pacific Rim Index and CAT.

Tokyo	Jan	Feb	Mar	Apr	May	Jun	Jul	Aug
Bloomberg	209.5	219.0	308.9	450	592.0	682.0	818.0	855.0
Temperature	225.0	225.0	305.0	479.0	623.0	679.0	812.0	823.0
Osaka	Jan	Feb	Mar	Apr	May	Jun	Jul	Aug
Bloomberg	200.2	220.8	301.9	460	627.0	716.0	861.0	899.0
Temperature	181.0	215.0	298.0	464.0	621.0	726.0	843.0	878.0

Table1.2 Tokyo & Osaka Temperature Index in 2009

For a further study on the Pacific Rim Index, we found certain characteristic of it, which is different from the common properties of HDD,CDD and CAT:

Firstly, instead of 20 local currency multiplied by the degree day index, the contract size measures with 2,500 Japanese Yen.

Secondly, the contracts are issued and traded following a cycle instead of 2 seasons in a year , which means there are 12 contracts per year with measurement period of each month of the specific year.

2.2.2 Pacific Rim Index in CME

Pacific Rim Index are shown with certain notations that are being used for traders to identify the measurement period of certain contract: F for January, G for February, H for March, J for April, K for May, M for June, N for July, Q for August, U for September, V for October, X for November and Z for December. For abbreviation, F9 defines the contract with measurement period of January,2009.

Trading-Period			Measurement-Period	
Code	First-trade	Last-trade	τ_1	τ_2
F9	20080203	20090202	20090101	20090131
G9	20080303	20090302	20090201	20090228
H9	20080403	20090402	20090301	20090331
J9	20080503	20100502	20090401	20090430
K9	20080603	20090602	20090501	20090531
M9	20080703	20090702	20090601	20090630
N9	20080803	20090802	20090701	20090731
Q9	20080903	20091002	20090801	20090831
U9	20081003	20091102	20090901	20090930
V9	20081103	20091202	20091001	20091030
X9	20081203	20091202	20091101	20091130
Z9	20090103	20100102	20091201	20091231

Table 1.3: Tokyo & Osaka Pacific Rim Index listed on CME

Table 1.2 shows the Pacific Rim Index being traded on CME. According to the information released in CME, the trading of 1 specific contract terminates 2 calender days after the expiration of the contract month. The cash settlement of the contract is based on the specified degree day index 2 calendar days after the future contract month.

Figure 1 shows the dynamics of index futures of Tokyo and Osaka on April 1st, 2009. The green line denotes contracts of Tokyo, while the red one is contracts of Osaka.

All of the contracts being traded on this day are plotted, where we can see a high price for contract for the season with high temperature, and low price for contract with measurement period in cool season.

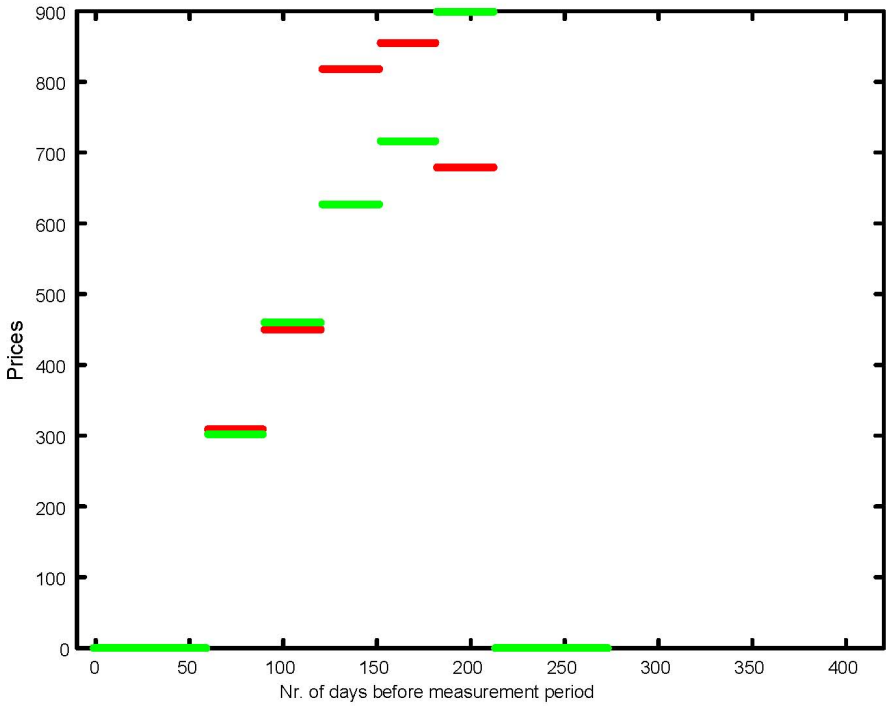

Figure 1 CME Pacific Rim Index: Tokyo (green) & Osaka (red) contracts J9 to J0, source: Bloomberg 20090402

However, as Asia Pacific region is a new market, the associated data of trading, volume and price of Pacific Rim Index, provided in Bloomberg is very limited.

Firstly, no trading information before October, 2008 was recorded in Bloomberg. For example, we could not find contracts with names Z7, F8, G8,..., which means the contract with measurement period of Dec.2007, Jan,2008 and Feb.2009 on Bloomberg.

Secondly, limited by our temperature data which is due to Aug.31, 2009, we could not price contracts with measurement period after August,2009.

Thirdly, Bloomberg reports only settled price for contract F9,G9 and H9 instead of the detailed trading information. The possible reason could be a limit of space in its data portal, as detailed trading information is available for maximal of 7 contracts in Bloomberg.(see Bloomberg professional service: description of M3 Index.)

	M31	M32	M33	M34	M35	M36	M37	M38	M39	M310
200810	V8	X8	Z8	F9	G9	H9	J9	K9	M9	N9
200811	X8	Z8	F9	G9	H9	J9	K9	M9	N9	Q9
200812	Z8	F9	G9	H9	J9	K9	M9	N9	Q9	U9
200901	F9	G9	H9	J9	K9	M9	N9	Q9	U9	V9
200902	G9	H9	J9	K9	M9	N9	Q9	U9	V9	X9
200903	H9	J9	K9	M9	N9	Q9	U9	V9	X9	Z9
200904	J9	K9	M9	N9	Q9	U9	V9	X9	Z9	F0
200905	K9	M9	N9	Q9	U9	V9	X9	Z9	F0	G0
200906	M9	N9	Q9	U9	V9	X9	Z9	F0	G0	H0
200907	N9	Q9	U9	V9	X9	Z9	F0	G0	H0	J0
200908	Q9	U9	V9	X9	Z9	F0	G0	H0	J0	K0
200909	U9	V9	X9	Z9	F0	G0	H0	J0	K0	M0
200910	V9	X9	Z9	F0	G0	H0	J0	K0	M0	N0
200911	X9	Z9	F0	G0	H0	J0	K0	M0	N0	Q0
200912	Z9	F0	G0	H0	J0	K0	M0	N0	Q0	U0

Table 1.4: Tokyo Contracts' availability during 20081001-20090831 shown with names.Blue and Dark blue parts of the matrix are not available in the data set. The white part of the contracts are taken into consideration in pricing part.

Table 1.4 shows the availability of Tokyo's contracts. The trading information of 5 contracts, namely J9,K9,M9,N9 and Q9, during period between 20081001 and 20090831 (the white part in Table 1.4) are considered, in terms of the problem reported above. M31,...M310 denotes the generic that the contracts are grouped into. Tokyo has 10 generic, contracts grouped in the first generic has the measurement period of the months that the contracts are being traded, while those in the second generic has measurement periods with one month ahead.

Addressing the trading information of Osaka's weather derivative, Bloomberg reports 1 generic with simplification. By a detailed checking with contract names, we obtained the trading information of the 5 contracts, J9,K9, M9, N9 and Q9 between 20081001 and 20090831 shown by Table 1.5.

Date	Contracts traded				
200810	J9	K9	M9	N9	Q9
200811	J9	K9	M9	N9	Q9
200812	J9	K9	M9	N9	Q9
200901	J9	K9	M9	N9	Q9
200902	J9	K9	M9	N9	Q9
200903	J9	K9	M9	N9	Q9
200904	J9	K9	M9	N9	Q9
200905		K9	M9	N9	Q9
200906			M9	N9	Q9
200907				N9	Q9
200908					Q9

Table 1.5 Osaka Contracts' availability 20081001-20090831.

3 Dynamics of Temperature

In this section, we are going to define a general continuous-time autoregressive model, which could be fit to the temperature data observed in Asia.

3.1 CAR model

Continuous-time Autoregressive model is an analogue of an Autoregressive time series. It was firstly studied by Philips (1959), then applied to temperature data, with an aim of pricing the weather derivative, by Benth et al 2007.

Let $X_t \in \mathbb{R}^p$: With the definition of the vectorial Ornstein-Uhlenbeck equation

$$dX_t = AX_t dt + e_{pt}\sigma_t dB_t \tag{4}$$

e_k:k'th unit vector in $\mathbb{R}^p$ for $k = 1, ...p, \sigma_t > 0$
B_t:Brownian motion; A: $p \times p$-matrix

$$\mathbf{A} = \begin{pmatrix} 0 & 1 & 0 & \dots & 0 \\ 0 & 0 & 1 & \dots & 0 \\ \vdots & & \ddots & & \vdots \\ 0 & \dots & \dots & 0 & 1 \\ -\alpha_p & -\alpha_{p-1} & \dots & & -\alpha_1 \end{pmatrix} \tag{5}$$

Solution of $X_t = x \in \mathbb{R}^p$:

$$X_s = exp\{A(s-t)\}x + \int_s^t exp\{A(s-u)\}e_p\sigma_u dB_u \tag{6}$$

X_q can be the $q'th$ coordinate of the vector X with $q = 1, ...p$, in the temperature time series:

$$T_t = \Lambda_t + X_{1t} \tag{7}$$

X_{1t} is a Markov process, X_q is a discretization of the CAR model.By substituting iteratively into the discrete-time dynamics, the discrete version of the CAR(p) process could be written as following(Benth et al 2007): For $p = 1$,

$$dX_{1t} = -\alpha_1 X_{1t} dt + \sigma_t dB_t \tag{8}$$

For $p = 2$,

$$\begin{aligned} X_{1(t+2)} \approx\ & (-\alpha_1 + 2) X_{1(t+1)} \\ & + (\alpha_1 - \alpha_2 - 1) X_{1(t)} + \sigma_t (B_{t-1} - B_t) \end{aligned} \tag{9}$$

For $p = 3$,

$$\begin{aligned} X_{1(t+3)} \approx\ & (-\alpha_1 + 3) X_{1(t+2)} \\ & + (2\alpha_1 - \alpha_2 - 3) X_{1(t+1)} \\ & + (-\alpha_1 + \alpha_2 - \alpha_3 + 1) X_{1(t)} + \sigma_t d(B_{t-1} - B_t) \end{aligned} \tag{10}$$

For $p = 4$,

$$\begin{aligned} X_{1(t+4)} \approx\ & (-\alpha_1 + 4) X_{1(t+3)} \\ & + (3\alpha_1 - \alpha_2 - 6) X_{1(t+2)} \\ & + (-3\alpha_1 + 2\alpha_2 + 4) X_{1(t+1)} \\ & + (\alpha_1 - \alpha_2 + \alpha_3 - \alpha_4 - 1) X_{1(t)} + \sigma_t d(B_{t-1} - B_t) \end{aligned} \tag{11}$$

...

For $p = 10$,

$$
\begin{aligned}
Y_{1(t+10)} \approx\ & (-\alpha_1 + 10)Y_{1(t+9)} \\
& + (9\alpha_1 - \alpha_2 - 11)Y_{1(t+8)} \\
& + (-36\alpha_1 + 8\alpha_2 + 64)Y_{1(t+7)} \\
& + (78\alpha_1 - 24\alpha_2 + \alpha_3 - \alpha_4 - 204)Y_{1(t+6)} \\
& + (-97\alpha_1 + 37\alpha_2 - 6\alpha_3 - 2\alpha_4 + 229)Y_{1(t+5)} \\
& + (69\alpha_1 - 34\alpha_2 + 15\alpha_3 + \alpha_4 + 2\alpha_5 - \alpha_6 - 166)Y_{1(t+4)} \\
& + (-17\alpha_1 + 6\alpha_2 - 8\alpha_4 + 3\alpha_5 - 2\alpha_6 + \alpha_7 + 44)Y_{1(t+3)} \\
& + (-3\alpha_1 + 4\alpha_2 - 6\alpha_3 + 5\alpha_4 - \alpha_5 + \alpha_7 - \alpha_8 + 9)Y_{1(t+2)} \\
& + (-3\alpha_1 + 5\alpha_2 + 6\alpha_4 - 5\alpha_5 + 4\alpha_6 - 3\alpha_7 + 2\alpha_8 + 5)Y_{1(t+1)} \\
& + (\alpha_1 - \alpha_2 + \alpha_3 - \alpha_4 + \alpha_5 - \alpha 6 + \alpha_7 - \alpha_8 + \alpha 9 - \alpha_{10} - 1)Y_{1(t)} + \sigma_t d(B_{t-1} - B_t)
\end{aligned}
\tag{12}
$$

...
For $p = 13$,

$$
\begin{aligned}
Y_{1(t+13)} \approx\ & (-\alpha_1 + 13)Y_{1(t+12)} \\
& + (12\alpha_1 - \alpha_2 - 22)Y_{1(t+11)} \\
& + (-66\alpha_1 + 9\alpha_2 + 64)Y_{1(t+10)} \\
& + (52\alpha_1 - 49\alpha_2 - \alpha_3 + \alpha_4 + 139)Y_{1(t+9)} \\
& + (-136\alpha_1 + 134\alpha_2 - 9\alpha_3 + \alpha_4 + 767)Y_{1(t+8)} \\
& + (475\alpha_1 - 225\alpha_2 + 31\alpha_3 + 4\alpha_4 + 2\alpha_5 - \alpha_6 - 1403)Y_{1(t+7)} \\
& + (-593\alpha_1 + 175\alpha_2 - 64\alpha_3 - 17\alpha_4 - 3\alpha_5 + \alpha_6 + \alpha_7 + 1434)Y_{1(t+6)} \\
& + (352\alpha_1 - 25\alpha_2 + 27\alpha_3 + 35\alpha_4 - 4\alpha_5 + 3\alpha_6 - 2\alpha_7 - \alpha_8 - 850)Y_{1(t+5)} \\
& + (-144\alpha_1 - 8\alpha_2 + 15\alpha_3 - 108\alpha_4 + 5\alpha_5 - 9\alpha_6 + 3\alpha_7 + 5\alpha_8 + 276)Y_{1(t+4)} \\
& + (10\alpha_1 - 15\alpha_2 + \alpha_3 - 136\alpha_4 + 10\alpha_5 + 7\alpha 6 + 12\alpha_7 - 14\alpha_8 + \alpha_9 - \alpha_{10} - 33)Y_{1(t+3)} \\
& + (-\alpha_1 - 11\alpha_2 - 15\alpha_3 - 13\alpha_4 - 17\alpha_5 + 3\alpha 6 - 12\alpha_7 + 14\alpha_8 + 3\alpha_9 + 3\alpha_{10} - \alpha_{11} \\
& + 7)Y_{1(t+2)} + (6\alpha_1 - 7\alpha_2 + 9\alpha_3 - 8\alpha_4 + 8\alpha_5 - 5\alpha 6 + 6\alpha_7 - 5\alpha_8 + 3\alpha_9 - 3\alpha_{10} - 2\alpha_{11} \\
& - \alpha_{12} - 5)Y_{1(t+1)} + (-\alpha_1 + \alpha_2 - \alpha_3 + \alpha_4 - \alpha_5 + \alpha_6 - \alpha_7 + \alpha_8 - \alpha_9 + \alpha_{10} - \alpha_{11} \\
& + \alpha_{12} - \alpha 13 + 1)Y_{1(t)} + \sigma_t d(B_{t-1} - B_t)
\end{aligned}
\tag{13}
$$

3.2 Model for Temperature

Let T_t be average temperature in day t, which consists a seasonal component.

$$T_t = \Lambda_t + X_t \tag{14}$$

Λ is a deterministic seasonal function,and has the form:

$$\Lambda_t = a + bt + c \cdot \cos\{2\pi(t-d)/365\} \tag{15}$$

X_t is a p-order autoregressive process of the form:

$$X_t = \beta_0 + \sum_{i=1}^{p} \beta_i X_{t-i} + \sigma_t \varepsilon_t \tag{16}$$

where ε_t is white noise and σ_t follows:

$$\begin{aligned}\sigma_t^2 = c_1 + \sum_{j=1}^{16} \{c_{2j}\cos(2j\pi t/365) + c_{2j+1}\sin(2j\pi t/365)\} \\ + \alpha_1(\sigma_{t-1}\varepsilon_{t-1})^2 + \beta_1\sigma_{t-1}^2\end{aligned} \tag{17}$$

A high order of 16 is chosen after comparison with results from lower order of 2,4,...14; GARCH(1,1) is selected with reference from AIC and BIC.

3.3 Empirical Analysis of Temperature in Asia

In this section, we will study the temperature dynamics for 4 cities in Asia: Tokyo, Osaka,Taipei and Beijing. The first two cities' temperature has been enlisted as index in Chicago Mercantile Exchange,while the last two cities' temperature are analyzed in terms of their geographical and meteorological relevance to the temperature of the 2 Japanese cities, as well as the possibility of a further studies over a joint analysis of the derivative pricing.

The temperature data was obtained from the Bloomberg Professional service.Tokyo,

Osaka and Beijing's temperature datasets contain observations of 36.5 years from 19730101 to 20090831; while Taipei's data has a later starting point of 19920101.

In order to assure the quality of the data from Bloomberg, we consult on Japanese Meteorological Agency (JMA) for a double check. Table 2.1 has listed the differences between data from Bloomberg and from JMA. By common sense, it is easily detected that Bloomberg reports data with obvious deviation from fact. For example, while Tokyo's annual average temperature is around 16^oC,and the average temperature in January in the total dataset is around 5^oC, the temperature of 18^oC on Jan.14,1996 reported from Bloomberg should be incorrect compared with a 8^oC by JMA.On the other side, Osaka's data was also checked with respect to the information provided by JMA, Table 2.2 shows the comparison result, indicating that Bloomberg has been providing bad data, which clusters in year 1998.After being proved as unreasonable, bad data were corrected with reference from the JMA.

Date	Bloomberg	JMA
20080921	13	23
20080918	14	24
20080705	16	26
20080628	13	23
20070906	16	26
20061004	12	22
19980214	5	13
19960114	18	8

Table 2.1:Check Tokyo's bad data with reference of JMA

Date	Bloomberg	JMA
19981014	13	23
19980930	15	25
19980905	13	23
19980801	16	26
19980517	13	23

Table 2.2:Check Osaka's bad data with reference of JMA

The statistical properties of the data from the 4 Asian cities differ with their variety of geographical locations. Interpreted from the descriptive statistics shown in Table 2.3, the 2 Japanese cities, Tokyo and Osaka's weather show a strong similarity, though Osaka has more volatile weather in terms of higher variance and standard deviation.Taipei warmer on average as it is located in tropical area. It also has the smallest variance and standard deviation,showing that the temperature does not deviate from the mean value and it is less volatile. Beijing, on the contrary, has a lower annual average temperature and the highest variance and standard deviation, showing the strongest volatility among all of the 4 cities in Asia. Though Beijing has a closer longitude with Tokyo, it has absolute different weather with Tokyo in terms its location as inland in China.

City	Nr.Obs	Mean	Median	Max	Min	Variance	Std
Tokyo	13329	16.21	16	33	-1	60.48	7.78
Osaka	13329	16.33	17	34	-4	72.79	8.54
Taipei	6453	23.74	24	34	8	34.06	5.48
Beijing	13329	12.73	14	36	-14	119.91	10.95

Table 2.3: Descriptive Statistics of 4 cities in Asia

Before proceeding to detailed modeling of the temperature, it is necessary that we get an overall view of the daily average temperature data of the 4 Asian cities. Through a glance over the total dataset of each city, we observe that the temperature fluctuates around a certain value all year around. Shown in Figure 2, a strong and unsurprising seasonality exists in the temperature of each city, showing that the daily average temperature moves repeatedly and regularly through periods of summer and winter.

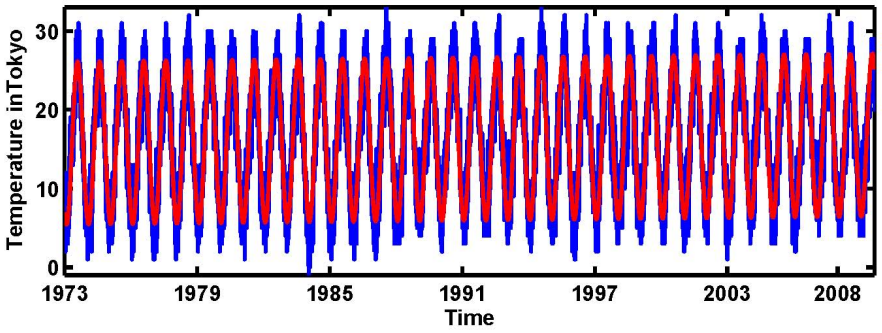
Temperature inTokyo
30
20
10
0
1973
1979
1985
1991
1997
2003
2008
Time

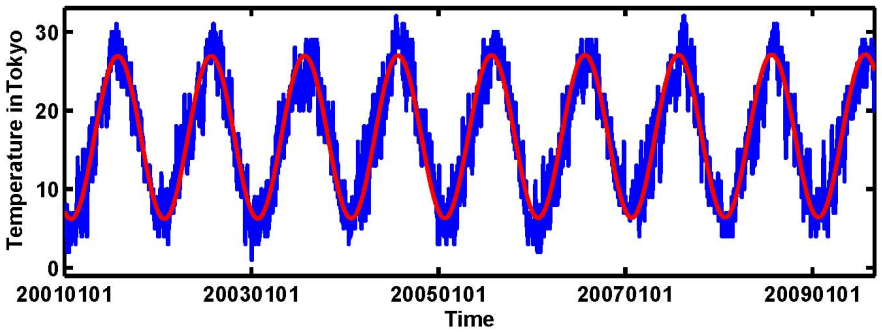
Temperature inTokyo
30
20
10
0
20010101
20030101
20050101
20070101
20090101
Time

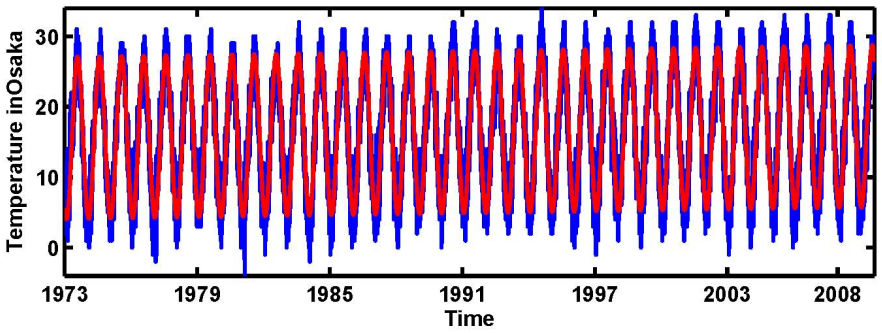
Temperature inOsaka
30
20
10
0
1973
1979
1985
1991
1997
2003
2008
Time

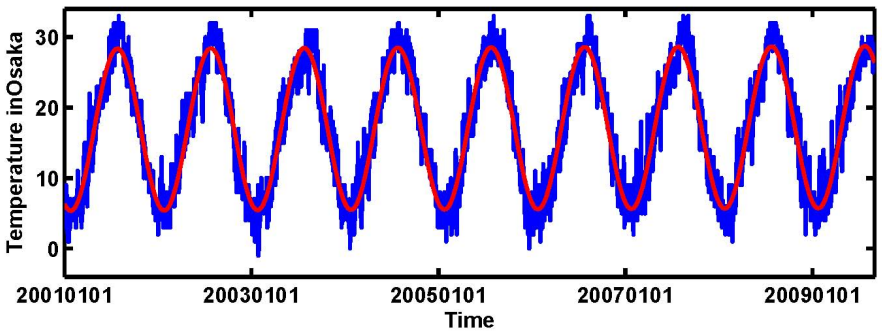
Temperature inOsaka
30
20
10
0
20010101
20030101
20050101
20070101
20090101
Time

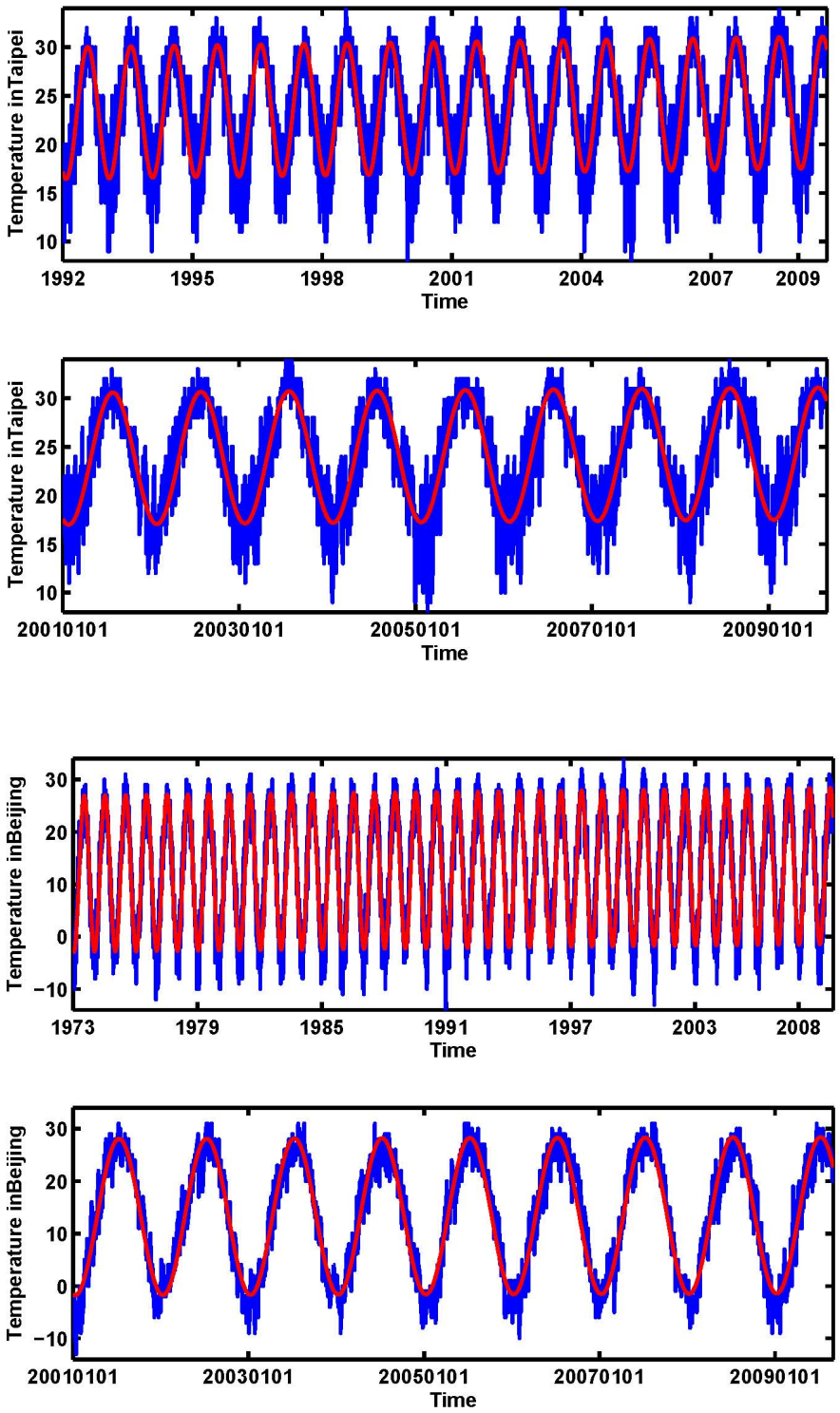

Figure 2 Daily average temperature of Tokyo, Osaka, Beijing 19730101-20081231 & Taipei 19920101-20090604 (upper panel)(blue line), as well as stretched plot

20010101-20081231(lower panel),Seasonality effect(red line) Source:Bloomberg

Thus, it is strongly suggested that we firstly decompose the temperature into a seasonality component and an non-seasonal part. Let T_t be average temperature in day t, which consists a seasonal component.

$$T_t = \Lambda_t + X_t \tag{14}$$

Λ is a deterministic seasonal function,and has the form:

$$\Lambda_t = a + bt + c \cdot \cos\{2\pi(t-d)/365\} \tag{15}$$

where a describes a linear trend; b means the increase of temperature with years,in another words, global warming; c describes the amplitude of the temperature's fluctuation, d is the parameter for the cycle.

The least squares fitted seasonal function with trend,as Equation 16, has captured the seasonality effectively by having the R^2 over 0.75 in 5% significant level for all of the 4 cities. Interpreted from the parameters shown in Table 2.2, we see that while Tokyo and Osaka has quite similar seasonality characteristics, Beijing has a lower trend, which is driven by the lower average temperature, already shown in the descriptive statistics. No strong global warming, denoted by $\hat{b}$ has been detected in any of the 4 cities.The amplitudes of temperature fluctuation differer among the cities. Beijing has an obviously bigger amplitude compared with others. The results could be explained intuitively with the geographical factors.

City	$\hat{a}$	$\hat{b}$	$\hat{c}$	$\hat{d}$
Tokyo	15.76	7.82e-05	10.35	-149.53
Osaka	15.54	1.28e-04	11.50	-150.54
Taipei	23.21	1.683e-03	6.782	-154.02
Beijing	11.97	1.18e-04	14.91	-165.51

Table 2.4 Estimated least squares fitted seasonal function

The lower panels of each subplot in Figure 2 show the stretched graph of the temperature in the previous 8.5 years, where the seasonality has been displayed by red lines.

After removing the seasonality as Equation 17 from the daily average temperatures, we try to model the left part by an AR(p) process. Before which, obviously, we need to check if the nonseasonal part X_t is a stationary process $I(0)$. Augmented Dickey-Fuller(ADF) Test as well as KPSS test are processed to check the stationarity of X_t in all of the 4 cities.

We assume that X_t is an AR(p) process, with $\{\beta_i\}_{i=0}^{p}$ autoregressive coefficients, can be rewritten:

$$\Delta X_t = \alpha X_{t-1} + \xi_1 \Delta X_{t-1} + \ldots + \xi_{p-1} \Delta X_{t-p+1} + \varepsilon_t \tag{18}$$

where $\alpha = \beta_1 + \beta_2 + \ldots + \beta_p - 1$ and $\xi_j = -(\beta_{j+1} + \beta_{j+2} + \ldots + \beta_p)$

Under H_0, α is 0 and there exists a unit root. With critical value as -2.57 at significant level of 1%, we see all of the 4 cities have rejected the null Hypothesis H_0, thus X_t in each of the Asian cities is stationary.

Data	Dickey-Fuller	Critical Value
Tokyo	-56.29	-2.57
Osaka	-17.86	-2.57
Taipei	-33.21	-2.57
Beijing	-20.40	-2.57

Table2.5 ADF test for nonseasonal part of 4 cities

KPSS test is applied to verify the stationarity of X_t. As a regression model with a time trend can be written as:

$$Y_t = c + \mu_t + k \sum_{i=1}^{t} \xi_i + \varepsilon_t \tag{19}$$

with stationary ε_t and $i.i.d\xi_i$ with an expected value 0 and variance 1. For $k \neq 0$ the process is integrated and for $k = 1$ trend stationary.

Under null hypothesis H_0, k is 0 and the process is not integrated.With p value smaller than 10%, we could not reject null hypothesis H_0 of stationarity.

Data	KPSS	P-value
Tokyo	0.091	< 0.1
Osaka	0.138	< 0.1
Taipei	0.067	< 0.1
Beijing	0.094	< 0.1

Table 2.6 KPSS test for nonseasonal part of 4 cities

With the justified stationarity of X_t in all of the 4 cities, we could proceed with the Autoregressive Process modeling.

$$Y_t = \beta_0 + \sum_{i=1}^{p} \beta_i Y_{t-i} + \sigma_t \varepsilon_t \tag{16}$$

In modeling the nonseasonal part of the temperatures by an AR(p) model, it is essential to decide the lag order p. Figure 3 shows the partial autocorrelation of the 4 time series. While an AR(3) is suggested by the plot of PACF, the BIC and AIC have suggested AR(10) for Tokyo, AR(13)for Osaka, AR(3)for Taipei and AR(12)for Beijing.

Table 2.5 shows the suggested lag orders as well as associated parameters $\hat{\beta}_i$. The first few lags,especially first 3 lags, for each of the cities show significant influences over the time series, while the parameters turn to drastically decrease as the lag order increases.

In terms of the high order of p and rather small estimated parameters, we check the stability of the moving windows of the time series by assuming that the variance is constant over each of the window.

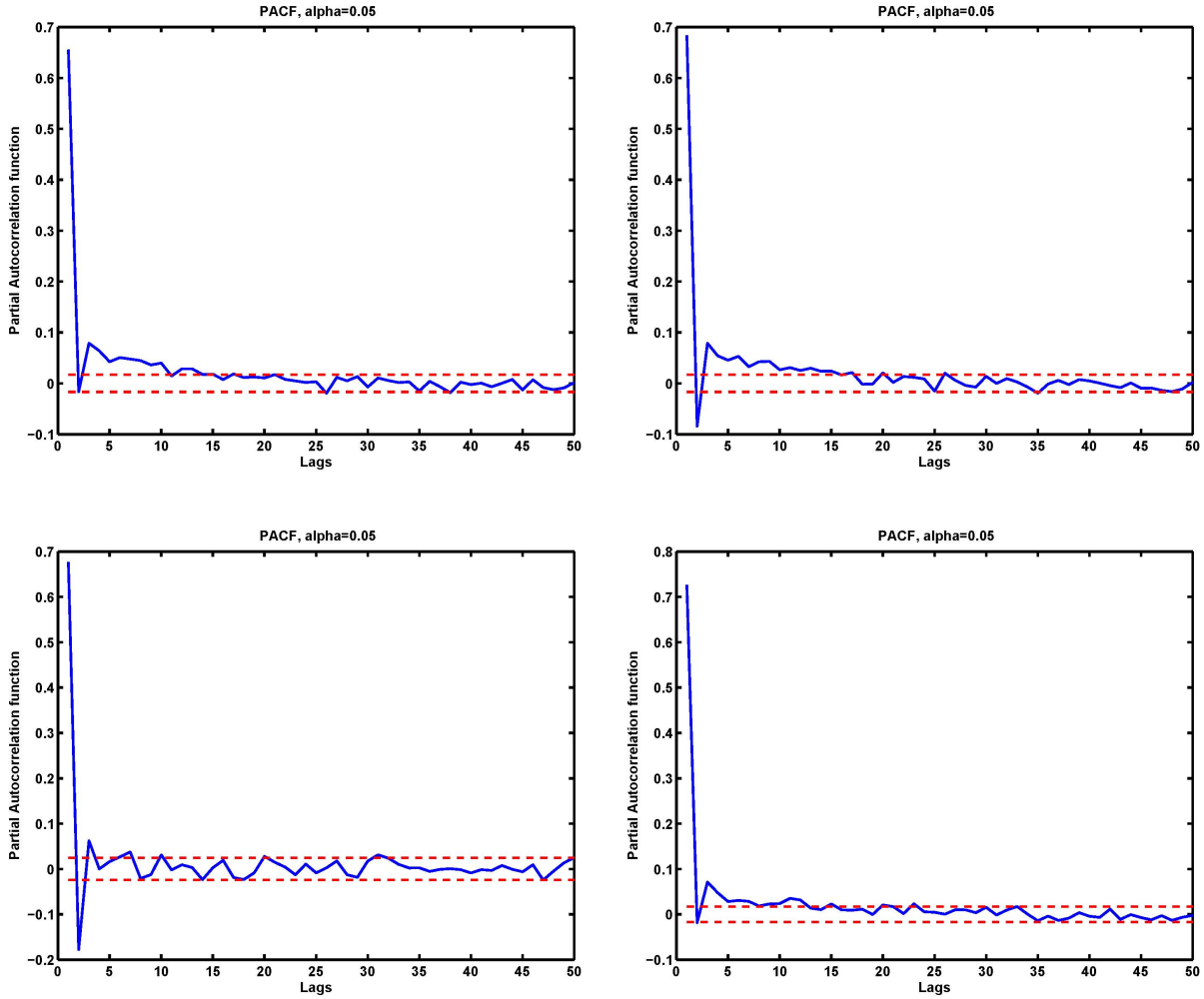

Figure 3: PACF of nonseasonal part of 4 Asian cities: Tokyo(upper left), Osaka(upper right), Taipei(lower left) & Beijing(lower right).

Parameters	Tokyo	Osaka	Taipei	Beijing
β_1	0.651	0.730	0.808	0.732
β_2	-0.071	-0.141	-0.228	-0.071
β_3	0.033	0.038	0.063	0.034
β_4	0.034	0.023		0.028
β_5	0.010	0.006		0.004
β_6	0.018	0.031		0.009
β_7	0.021	0.005		0.015
β_8	0.023	0.012		4.011e-04
β_9	0.011	0.027		0.008
β_{10}	0.040	0.006		-0.001
β_{11}		0.016		0.012
β_{12}		0.004		0.033
β_{13}		0.029		

Table 2.7 AR(p) suggested by AIC and BIC

Year	every 3 years	every 6 years	every 9 years	every 12 years	every 18 years
73-75	AR(1)	AR(3)	AR(3)	AR(8)*	AR(9)*
76-78	AR(1)				
79-81	AR(1)	AR(8)*			
82-84	AR(8)*				
85-87	AR(1)	AR(3)	AR(9)*	AR(3)	
88-90	AR(1)				
91-93	AR(1)	AR(3)	AR(3)		
94-96	AR(1)				
97-99	AR(1)	AR(1)	AR(3)	AR(3)	AR(3)
00-02	AR(1)				
03-05	AR(3)	AR(3)			
06-09	AR(1)				

Table 2.7 Check moving window for Tokyo.* denotes instability

Year	every 3 years	every 6 years	every 9 years	every 12 years	every 18 years
73-75	AR(1)	AR(3)	AR(3)	AR(3)	AR(6)*
76-78	AR(3)				
79-81	AR(3)	AR(3)			
82-84	AR(2)				
85-87	AR(3)	AR(3)	AR(3)	AR(6)*	
88-90	AR(3)				
91-93	AR(3)	AR(3)	AR(6)*		
94-96	AR(1)				
97-99	AR(2)	AR(2)	AR(3)	AR(7)*	AR(7)*
00-02	AR(1)				
03-05	AR(3)	AR(3)			
06-09	AR(1)				

Table 2.7 Check moving window for Osaka.* denotes instability

Year	every 3 years	every 6 years	every 9 years	every 12 years	every 18 years
91-93	AR(3)	AR(3)	AR(3)	AR(3)	AR(3)
94-96	AR(1)				
97-99	AR(2)	AR(2)	AR(3)		
00-02	AR(1)				
03-05	AR(3)	AR(3)			
06-09	AR(1)				

Table 2.7 Check moving window for Taipei.* denotes instability

Year	every 3 years	every 6 years	every 9 years	every 12 years	every 18 years
73-75	AR(1)	AR(3)	AR(3)	AR(3)	AR(6)*
76-78	AR(3)				
79-81	AR(1)	AR(2)			
82-84	AR(2)				
85-87	AR(3)	AR(3)	AR(3)	AR(6)*	
88-90	AR(3)				
91-93	AR(3)	AR(3)	AR(6)*		
94-96	AR(1)				
97-99	AR(1)	AR(1)	AR(5)*	AR(9)*	AR(9)*
00-02	AR(1)				
03-05	AR(3)	AR(3)			
06-09	AR(1)				

Table 2.7 Check moving window for Beijing.* denotes instability

By checking the stability of the moving windows in each of the time series, we identify that higher orders for AR is not stable, while AR(3) appears to be optimal for each of the 4 cities. Table 2.9 shows the parameters of AR(3) for all of the 4 cities in Asia.

AR(3)	β_1	β_2	β_3
Tokyo	0.668	-0.069	-0.079
Osaka	0.748	-0.143	0.079
Taipei	0.808	-0.228	0.063
Beijing	0.741	-0.071	0.071

Table 2.9 Parameters of AR(3) for 4 cities in Asia

After removing the seasonality and the trend components out of the time series, the residuals ε_t and squared residuals ε_t^2 of the AR(3)are plotted in the Figure 4.

The overview of the residuals of total data set has provided us with first glimpse of an important phenomenon: pronounced and persistent time-series volatility dynamics in the temperature shocks. In particular, the weather risk, as measured by its innovation variance, appears to be seasonal , as the amplitude of the residuals fluctuation varies over the course of each year, showing peaks in winter and summer. To gain additional insight into the strength and pattern of the conditional heteroscedasticity, we plot the correlograms of the squared residuals in Figure 5, taken to a maximum displacement of 1000 days. There is a clear evidence of strong nonlinear squared residuals dependence, driven by strong conditional variance dynamics.

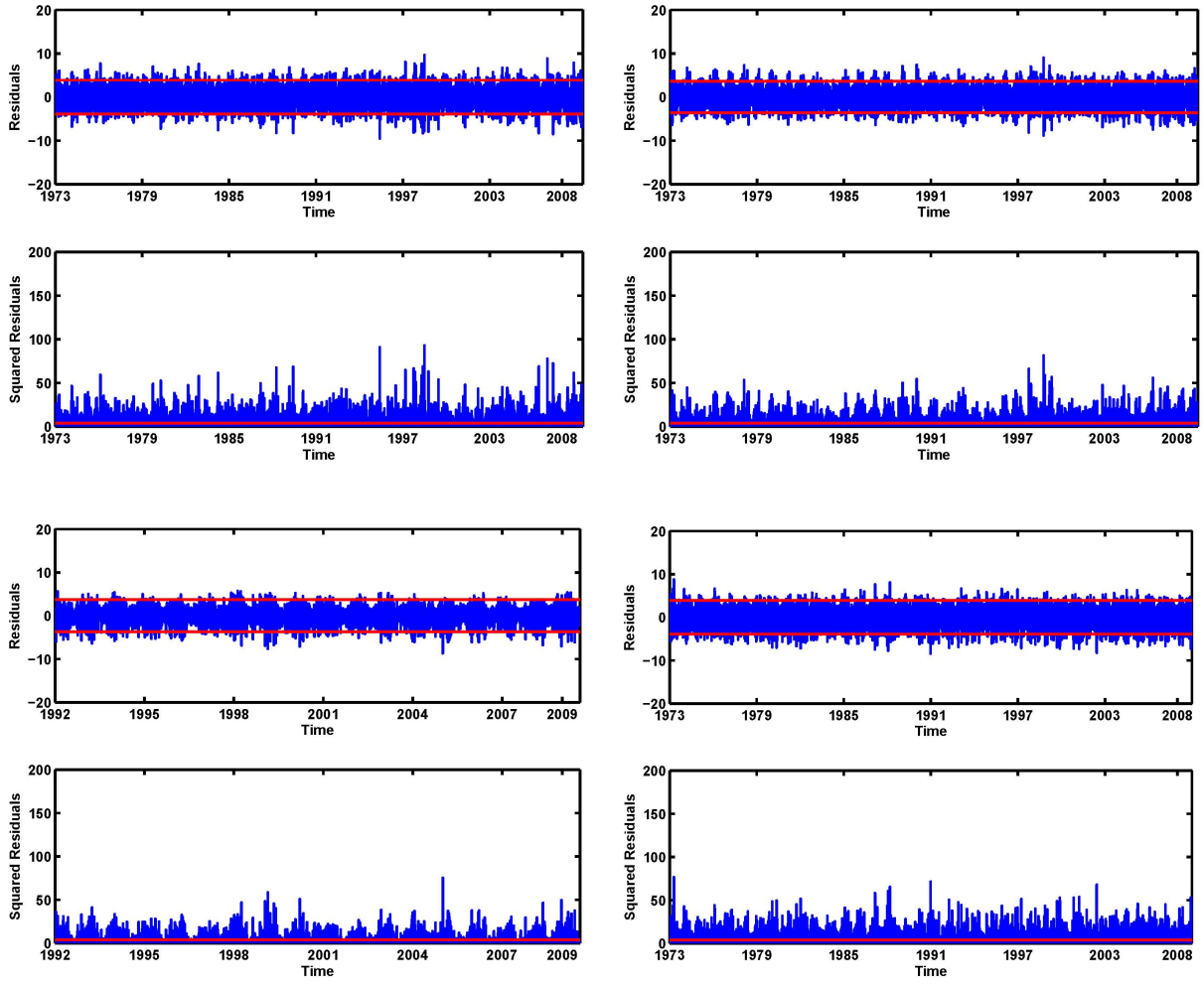

Figure 4 Residuals ε_t and squared residuals ε_t^2 in AR(3) of Tokyo (upper left),Osaka (upper right), Taipei (lower left), and Beijing (lower right), ε_t in the upper panel of each subplot, ε_t^2 of the AR(3) in the lower panel.

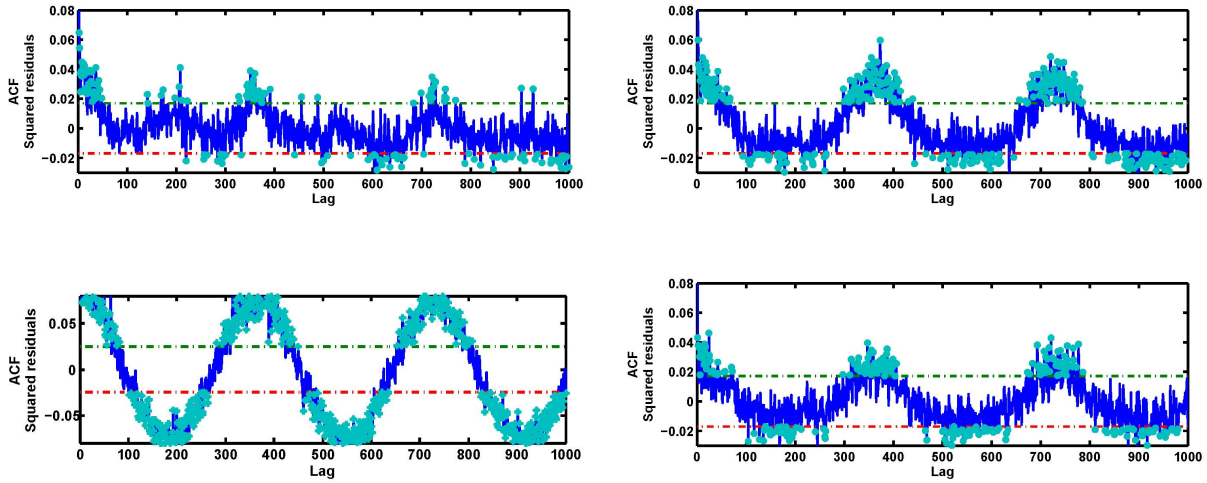

Figure 5: ACF of squared residuals ε_t^2 in AR(3) of Tokyo (upper left),Osaka (upper right), Taipei (lower left), and Beijing (lower right).

Thus, it is strongly suggested that we proceed the following modeling with a "2-Step Procedure", by firstly capturing the conditional mean dynamics with truncated fourier series and secondly applying GARCH model to obtain the conditional variance dynamics.

Firstly, we apply the truncated fourier series in order to capture the seasonal pattern in the volatility. Campbell et al.2005 has discussed 2 benefits of this application as it, on one side, can produce a smooth seasonal pattern, which accords with the basic intuition that progression through different seasons is gradual rather than discontinuous; and on the other hand, it promotes parsimony, which enhances numerical stability in estimation.

To apply truncated fourier series, we group the data into each of the day of one year, then take the variance and the expected value of the temperature of each day. We further apply the least square regression by fitting the truncated fourier series above. Figure 6 shows how the truncated fourier series captured the seasonal variance of the temperature of the 4 cities. A high order of 16 is chosen after comparing the residual sum of squared with lower orders of 2, 4, 6... The empirical results show that the higher the order is, the closer to normality the residual after being standardized is.

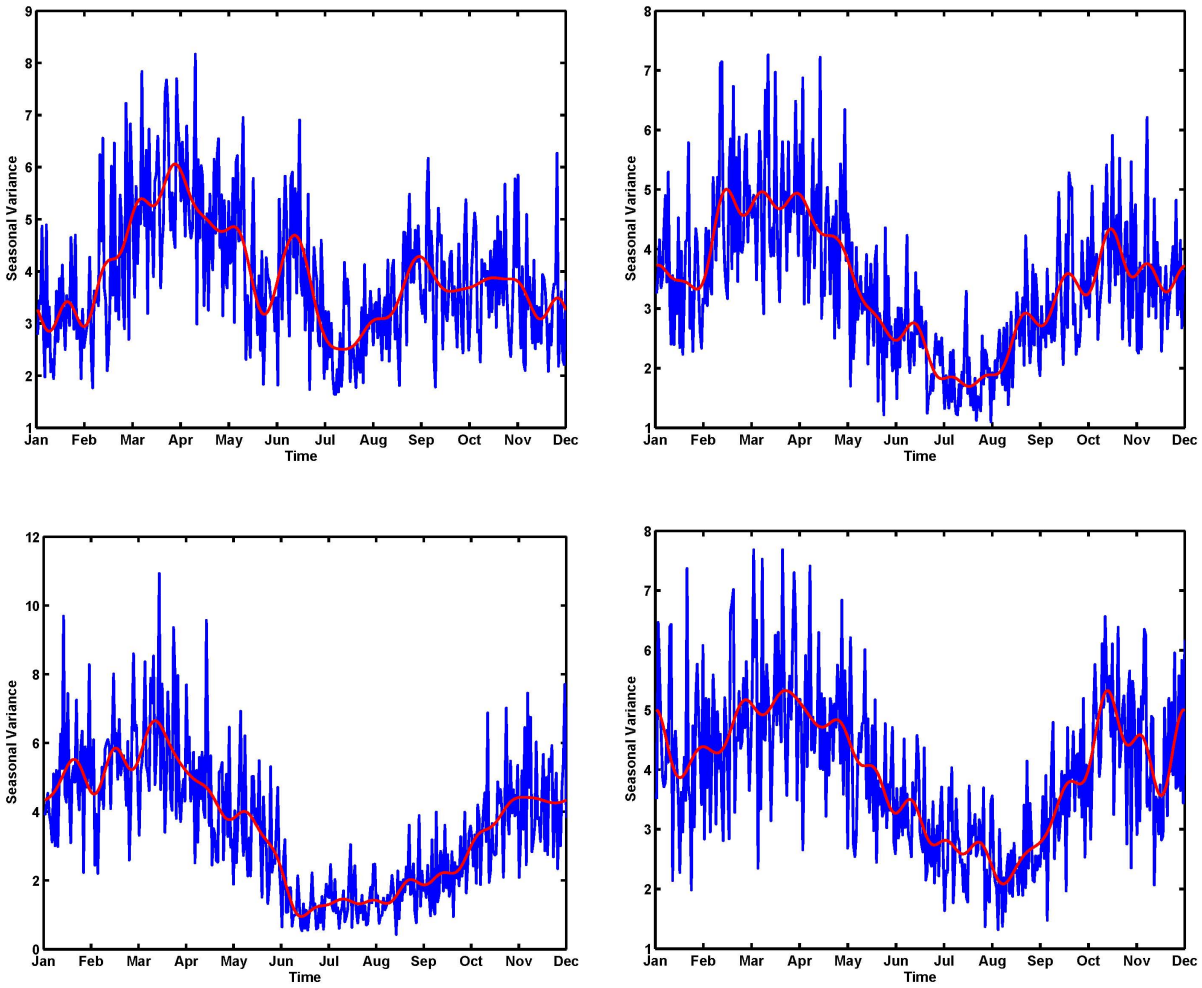

Figure 6: Seasonal Variance of Tokyo (upper left),Osaka (upper right), Taipei (lower left), and Beijing (lower right) with Truncated Fourier Series.

Interpreted from the result, we see that all of the cities show similarity by having a higher volatility in spring and lower volatility in summer; while Tokyo's temperature show a drastic change of seasonal variance in June.

Parameters	Tokyo	Osaka	Taipei	Beijing
c_1	3.91	3.40	3.54	3.95
c_2	-0.08	0.76	1.49	0.70
c_3	0.74	0.81	1.62	0.82
c_4	-0.70	-0.58	-0.41	-0.26
c_5	-0.37	-0.29	-0.19	-0.50
c_6	-0.13	-0.17	0.03	-0.20
c_7	-0.14	-0.07	-0.18	-0.17
c_8	0.28	0.01	-0.11	-0.05
c_9	-0.15	-0.04	-0.16	0.10
c_{10}	-0.21	-0.09	0.13	0.08
c_{11}	0.01	-0.04	0.11	0.07
c_{12}	0.13	0.12	-0.20	0.07
c_{13}	0.10	0.01	0.19	0.07
c_{14}	-0.10	0.07	0.03	0.10
c_{15}	0.04	0.02	0.01	0.07
c_{16}	0.21	0.11	-0.11	0.14
c_{17}	-0.02	0.01	0.02	-0.03
c_{18}	-0.19	0.02	0.01	0.01
c_{19}	0.06	0.07	-1.44	0.01
c_{20}	0.06	0.01	-0.03	0.03
c_{21}	-0.07	-0.02	0.11	-0.02
c_{22}	0.03	-0.11	-0.11	0.04
c_{23}	0.02	0.03	0.01	-0.02
c_{24}	-0.01	-0.05	-0.10	0.12
c_{25}	-0.08	0.10	-0.08	0.07
c_{26}	-0.02	-0.01	0.06	0.12
c_{27}	-0.01	0.03	-0.12	0.09
c_{28}	0.02	0.11	0.03	0.10
c_{29}	-0.09	-0.08	-0.04	-0.06
c_{30}	0.06	0.04	0.01	0.02
c_{31}	-0.08	0.01	-0.02	0.01
c_{32}	0.04	0.04	0.04	0.01
c_{33}	0.01	-0.01	0.08	-0.07

Table 2.10 Parameters of Truncated Fourier Series

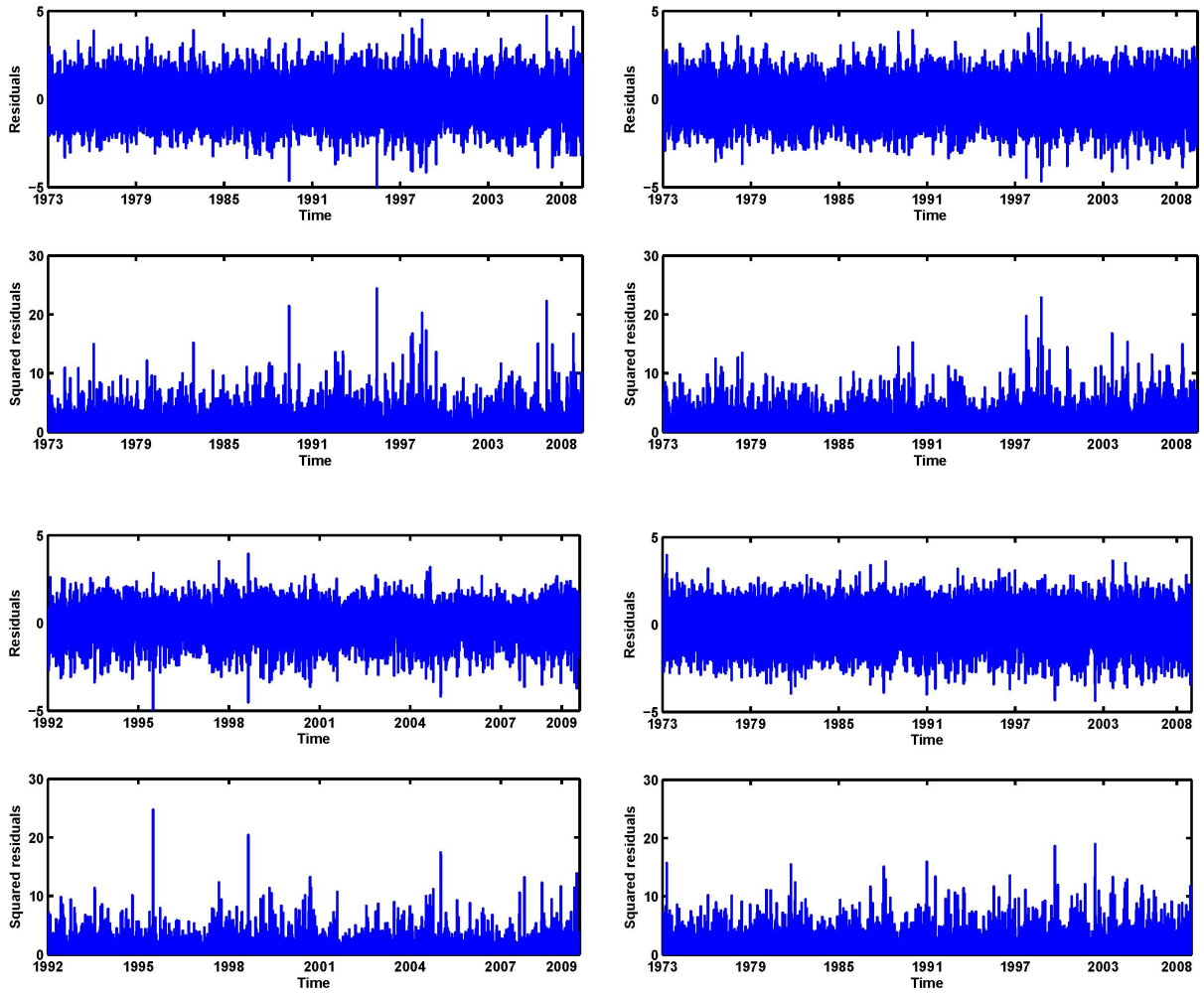

Figure 7: Residuals ε_t and squared residuals ε_t^2 of Tokyo (upper left),Osaka (upper right), Taipei (lower left), and Beijing (lower right) with Truncated Fourier Series.ε_t in the upper panel of each subplot, ε_t^2 of the AR(3) in the lower panel.

Secondly, in order to capture the conditional variance dynamics of residuals, we apply a GARCH(1,1) procedure by letting $\eta_t = \frac{\hat{\varepsilon}_t}{\sigma(t)}$ be the standardized residuals, h_t be the conditional variance of η_t:

$$h_t = \alpha_0 + \alpha_1 \eta_{t-1}^2 + \beta_1 h_{t-1} \tag{20}$$

GARCH(1,1)is chosen with the suggestion of AIC and BIC,presented by Table 2.9, where the result of applying GARCH(1,2), GARCH(2,1) and GARCH(2,2) are also listed. After comparison with respect to Akaike information criteria and Bayersian

information criteria, we see that GARCH(1,1) is optimal in this procedure.

AIC	GARCH(1,1)	GARCH(1,2)	GARCH(2,1)	GARCH(2,2)
Tokyo	3.7600e+4	3.7600e+4	3.7600e+4	3.7605e+4
Osaka	3.3730e+4	3.7732e+4	3.7734e+4	3.7734e+4
Taipei	1.8221e+3	1.8224e+3	1.8224e+3	1.8226e+3
Beijing	3.730e+4	3.7301e+4	3.7302e+4	3.7303e+4
BIC	GARCH(1,1)	GARCH(1,2)	GARCH(2,1)	GARCH(2,2)
Tokyo	3.7630e+4	3.7639e+4	3.7640e+4	3.7651e+4
Osaka	3.770e+4	3.770e+4	3.777e+4	3.778e+4
Taipei	1.8248e+3	1.8256e+3	1.8257e+3	1.8258e+3
Beijing	3.7329e+4	3.7338e+4	3.7339+4	3.7349e+4

Table 2.11 GARCH(1,1) selected with reference from AIC & BIC

City	$\hat{\alpha_1}$	$\hat{\beta_1}$
Tokyo	0.086	0.497
Osaka	0.040	0.522
Taipei	0.034	0.333
Beijing	0.063	0.337

Table 2.12 Coefficients of GARCH(1,1) of 4 cities

Table 2.12 reports the coefficients of GARCH(1,1). With the captured conditional variance by GARCH(1,1), we standardized the residuals $\frac{\hat{\varepsilon}_t}{\sigma(t)}$ with h_t, the residuals'correlograms plotted in Figure 8 with the maximum of 1000 days shows no more seasonal patterns or conditional variance dynamics.

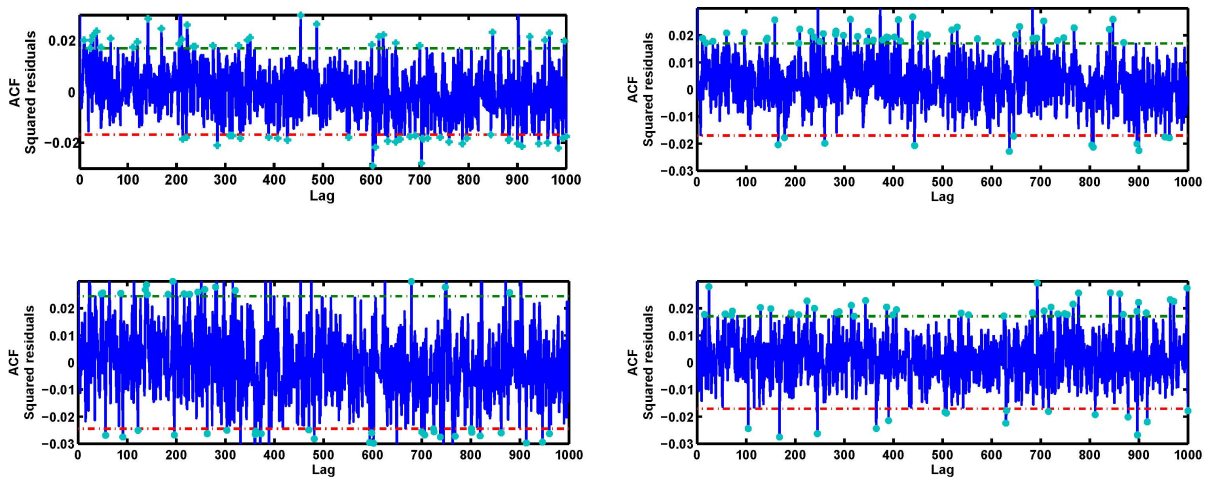

Figure 8: ACF of squared residuals ε_t^2 of Tokyo (upper left),Osaka (upper right), Taipei (lower left), and Beijing (lower right) standardized by Fourier and GARCH(1,1).

This result has strongly justified the effectiveness of our suggested "2-Step Approach". After the first step,we effectively captured the conditional mean dynamics with the truncated fourier series; after the second step with GARCH (1,1), we successfully removed the conditional variance dynamics out of our residuals. After twice standardization with volatility from the "2-Step Approach", the residuals becomes normal, shown in Figure 9.

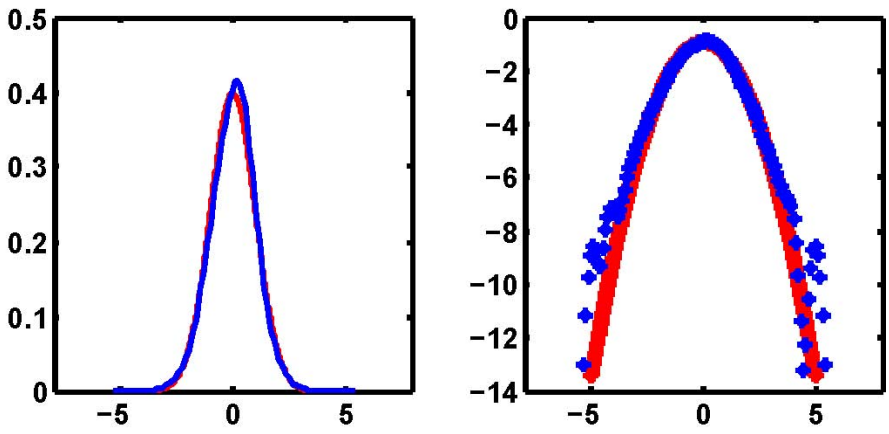

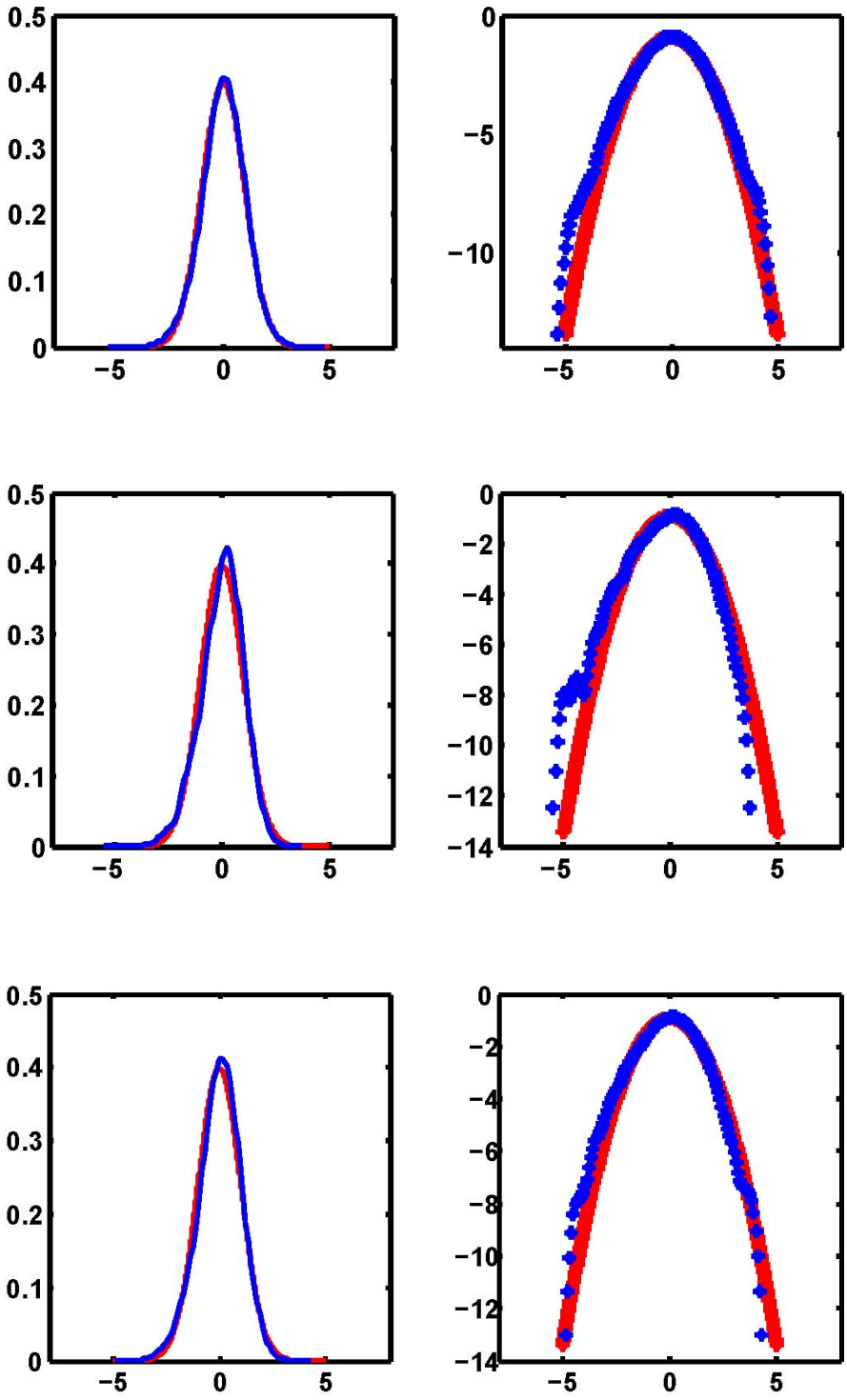

Figure 9: Kernel Density justifying normality of residuals standardized by truncated fourier series and GARCH(1,1). From up to down, Tokyo,Osaka, Taipei, Beijing

By achieving the Gaussian residuals, our continuous AR model is established with the parameters from table 2.11. Moreover, we are ready to proceed with the stochastic pricing of the temperature derivatives.

AR(3)	β_1	β_2	β_3
Tokyo	0.668	-0.069	-0.079
Osaka	0.748	-0.143	0.079
Taipei	0.808	-0.228	0.063
Beijing	0.741	-0.071	0.071
CAR(3)	α_1	α_2	α_3
Tokyo	2.332	1.734	0.323
Osaka	2.252	1.646	0.316
Taipei	2.192	1.611	0.357
Beijing	2.259	1.590	0.259
Eigenvalues	λ_1	λ_2	λ_3
Tokyo	-0.277+0.00i	-1.027+0.329i	-1.027-0.329i
Osaka	-0.295+0.00i	-0.978+0.336i	-0.978-0.336i
Taipei	-0.398+0.00i	-0.897+0.305i	-0.897-0.305i
Beijing	-0.231+0.00i	-1.014+0.304i	-1.014-0.304i

Table 2.13 Transformation from AR(3) to CAR(3)

3.4 Improved model with Local Linear Regression

In the previous subsection, we have achieved Gaussian residuals with "2-Step Approach" including both the truncated fourier series, as well as GARCH(1,1). Alternatively, a "1-Step Approach" using local linear regression performs even more effective, as it achieves normality with kernel smoothing regression.

$$m(x_0) = m(x) + m'(x)(x_0 - x) + \frac{m''(x)}{2}(x - x_0)^2 + \dots$$
$$\min_{a,b} \sum_{i=1}^{n} \Big(Y_i - a(x) - b(x)(X_i - x) \Big)^2 K(\frac{X_i - x}{h}) \tag{21}$$

We apply Epanichnikov kernel as the results standardized with it is closer to normality, compared with results using other kernels. The bandwidth is selected as optimal from the program. Shown as green solid line in Figure 10, we see that the kernel smoothing regression has captured the dynamics of the seasonal variance more effectively than the truncated fourier series, in terms of which the GARCH modeling is no more needed.

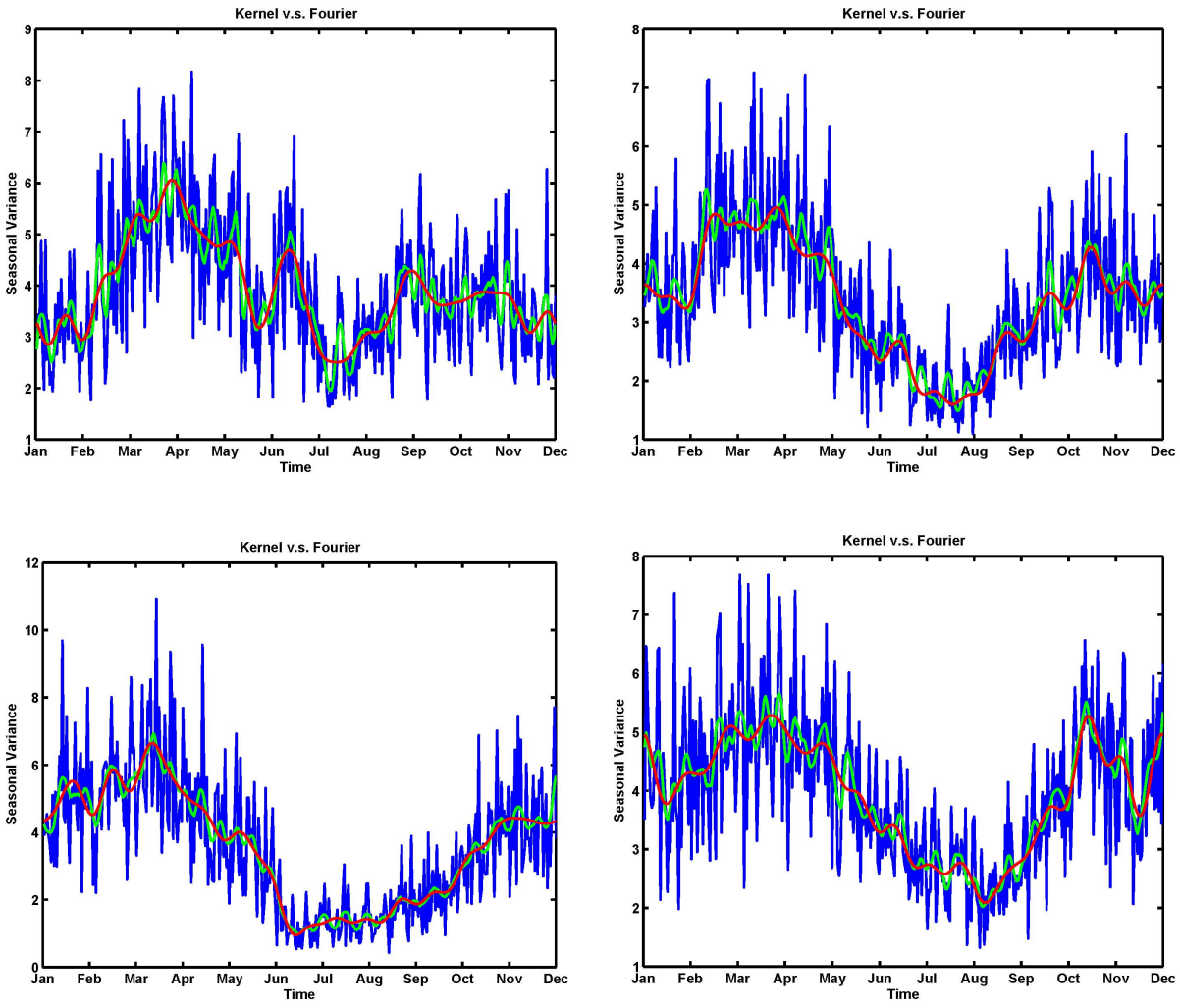

Figure 10: Seasonal Variance by Truncated Fourier Series (red) v.s. Kernel Smoothing Regression (green); Tokyo (upper left),Osaka (upper right), Taipei (lower left), and Beijing (lower right).

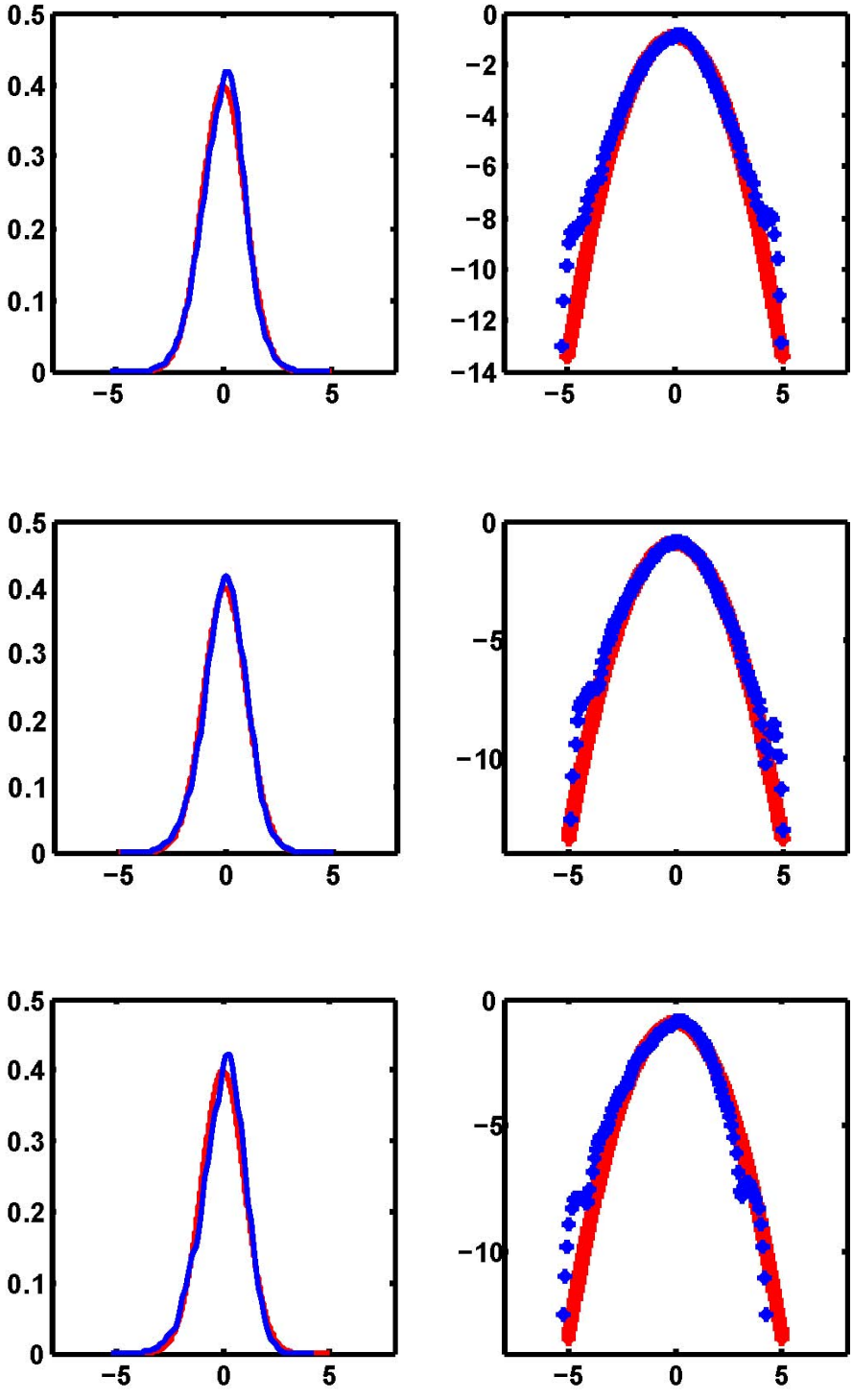
0.5
0.4
0.3
0.2
0.1
0
−5
0
5
0
−2
−4
−6
−8
−10
−12
−14
−5
0
5
0.5
0.4
0.3
0.2
0.1
0
−5
0
5
0
−5
−10
−5
0
5
0.5
0.4
0.3
0.2
0.1
0
−5
0
5
0
−5
−10
−5
0
5

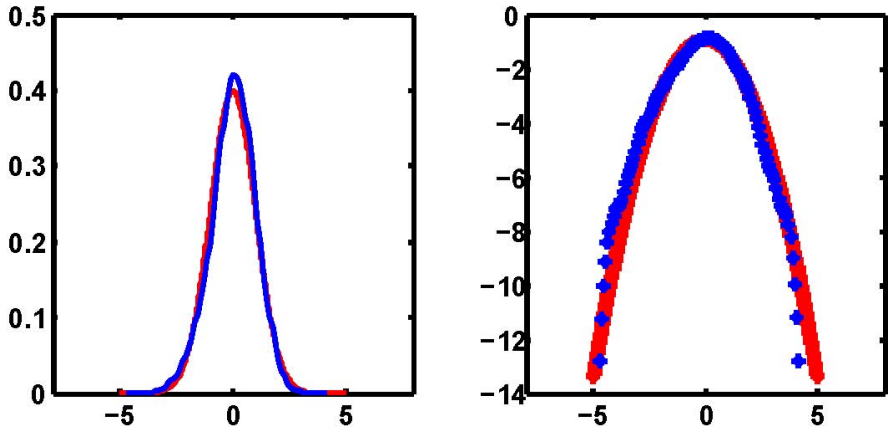

Figure 11: Kernel Density justifying normality of residuals standardized by smoothed seasonal variance from kernel regression.From up to down, Tokyo,Osaka, Taipei, Beijing

Tokyo	$\hat{\varepsilon}_t/\sigma_t^F$	$\hat{\varepsilon}_t/\sigma_t^F\sigma_t^G$	$\hat{\varepsilon}_t/\sigma_t^K$
Jacque Bera	158.00	127.23	114.50
Kurtosis	3.46	3.39	3.40
Skewness	-0.15	-0.11	-0.12
Osaka	$\hat{\varepsilon}_t/\sigma_t^F$	$\hat{\varepsilon}_t/\sigma_t^F\sigma_t^G$	$\hat{\varepsilon}_t/\sigma_t^K$
Jacque Bera	129.12	119.71	105.02
Kurtosis	3.39	3.35	3.33
Skewness	-0.15	-0.14	-0.14
Taipei	$\hat{\varepsilon}_t/\sigma_t^F$	$\hat{\varepsilon}_t/\sigma_t^F\sigma_t^G$	$\hat{\varepsilon}_t/\sigma_t^K$
Jacque Bera	201.09	198.40	184.17
Kurtosis	3.36	3.32	3.30
Skewness	-0.39	-0.39	-0.39
Beijing	$\hat{\varepsilon}_t/\sigma_t^F$	$\hat{\varepsilon}_t/\sigma_t^F\sigma_t^G$	$\hat{\varepsilon}_t/\sigma_t^K$
Jacque Bera	234.07	223.67	226.09
Kurtosis	3.28	3.27	3.25
Skewness	-0.29	-0.29	-0.29

Table 2.14: Statistics Comparison: Residual standardized by variances from Fourier function(F),GARCH(1,1)(G) and Kernel Smoothing (K).

Table 2.12 shows the comparison of the statistics in Normality test. Obviously, the "1-Step Approach" with smoothing technique has achieved an even more effective results. As the Gaussian residuals are achieved, we could apply financial mathematics and proceed with the stochastic pricing of temperature derivatives.

4 Temperature Derivative Pricing

In this section, we will firstly derive the future price formula for the contracts of Pacific Rim Index using the stochastic pricing model. Secondly, we will calibrate market price of risk from the real index on CME with different parametrization methods. At last, we will be estimating the prices with different MPR generated from different methods, then further derive the risk premier of temperature derivatives with respect to the case when MPR is equal to zero.

4.1 Future for Pacific Rim Index

We assume an arbitrage-free market for temperature derivatives. As temperature is not a tradable asset, the temperature derivative, which is written on the temperature index, is in lack of liquidity and completeness. In terms of this specific properties of temperature derivatives as well as that the future dynamics of temperature must be arbitrage-free, an equivalent measure Q is needed to be pinned down as a manageable class of pricing measure.

$\exists Q_{\theta_t}$ pricing so that:

$$F_{(t,\tau_1,\tau_2)} = E^{Q_{\theta_t}}[Y_t|F_t] \tag{22}$$

by Girsanov Theorem:

$$B_t^\theta = B_t - \int_0^t \theta_u du \tag{23}$$

θ_t is real valued,bounded,piecewise continuous function

The existence of Q_{θ_t} has made B_t^θ a Brownian motion for $t \in [0, \tau_m ax]$. Therefore, the dynamics of temperature X_t could be written under Q^θ as:

$$dX_t = (AX_t + e_p \sigma_t \theta_t)dt + e_p \sigma_t dB_t^\theta \tag{24}$$

for $s \geq t \geq 0$:

$$X_s = exp\{A(s-t)\}x + \int_s^t exp\{A(s-u)\}e_p\sigma_u\theta_u du + \int_s^t exp\{A(s-u)\}e_p\sigma_u dB_u \tag{25}$$

Previously, we have shown that Pacific Rim Index has a strong similarity with cumulated average temperautre (CAT), which suggests us apply the CAT formula in pricing the Pacific Rim Index contracts :

$$CAT(\tau_1, \tau_2) = \int_{\tau_1}^{\tau_2} T(t)dt \tag{3}$$

By incorporating the pricing measure Q^θ, the future of CAT could be written as:

$$\begin{aligned} F_{CAT(t,\tau_1,\tau_2)} &= E^{Q_\theta}[\int_{\tau_1}^{\tau_2} T_s ds|F_t] \\ &= \int_{\tau_1}^{\tau_2} \Lambda_u du + a_{t,\tau_1,\tau_2}X_t + \int_t^{\tau_1} \theta_u\sigma_u a_{t,\tau_1,\tau_2}e_p du \\ &+ \int_{\tau_1}^{\tau_2} \theta_u\sigma_u e_1^\top A^{-1}[exp\{A(\tau_2-u)\} - I_p]e_p du \end{aligned} \tag{26}$$

$$a_{(t,\tau_1,\tau_2)} = e_1^\top A^{-1}[exp\{A(\tau_2-t)\} - exp\{A(\tau_1-t)\}] \tag{27}$$

I_p:is a pxp Identity Matrix

4.2 Infer MPR $\hat{\theta}_t^i$

Previously, we have introduced the necessity for adopting an equivalent pricing measure Q^θ. In order to deal with the illiquidity and incompleteness of the market for weather derivatives, we need to estimate the market price of risk, with which the individual's attitudes towards risk is no longer sensitive in our pricing and hedging procedure. Market Price of Risk is a new parametrization which could be calibrated from the data of the real market and further be applied to pin down an estimated price. Thus, in this section, we will be inferring the MPR from the real index on

CME market by considering both cases when MPR is constant for contract in each trading day and when MPR is time dependent.

4.2.1 Constant MPR for each contract per trading day

Firstly we assume that MPR $\hat{\theta}_t^i$ is constant for all maturities for each contract. By inverting Equation (21), we could infer $\hat{\theta}_t^i$ for contracts with trading date $t < \tau_1 < \tau_2$.

Assume $\hat{\theta}_t^i$ is constant for each i contract, $i = 1, 2, 3, ...12$

$$\begin{aligned}\arg\min_{\hat{\theta}_t^i} = \Bigg(& F_{CAT(t,\tau_1^i,\tau_2^i)} - \int_{\tau_1^i}^{\tau_2^i} \hat{\Lambda}_u du - \hat{a}_{t,\tau_1^i,\tau_2^i} \hat{X}_t \\ & - \hat{\theta}_t^i \{ \int_t^{\tau_1^i} \hat{\sigma}_u \hat{a}_{t,\tau_1^i,\tau_2^i} e_p du \\ & + \int_{\tau_1^i}^{\tau_2^i} \hat{\sigma}_u e_1^\top A^{-1} [exp\{A(\tau_2^i - u)\} - I_p] e_p du) \} \Bigg)^2 \end{aligned} \tag{28}$$

The middle part of Figure 12 and lower part of Figure 13 has shown the MPR of 5 contracts being traded on 20090402 for both of the 2 cities.It is obvious that the contracts' MPR have been strongly influenced by the temperature variation σ_t.

In the case of Tokyo, On the date of 20090402,contract J9,highlighted as red, has an MPR around 0; contract K9(green)and M9(pink)'s MPR jumps to negative as the seasonal variance from May to June decrease drastically; the MPR of contract N9(purple) and Q9(blue)jumps back to positive again as the seasonal variance during July to August increases rapidly.

Similarly, Osaka's seasonal variances' changes have been obviously reflected from their MPR of different contracts. Further,by a comparison between Tokyo and Osaka's MPR, we see an even more drastic change in Osaka's MPR,with the smallest MPR lower than -0.5.This could be explained by the bigger amplitude of Osaka's seasonal variance's fluctuation compared with Tokyo's, shown by Figure 5.

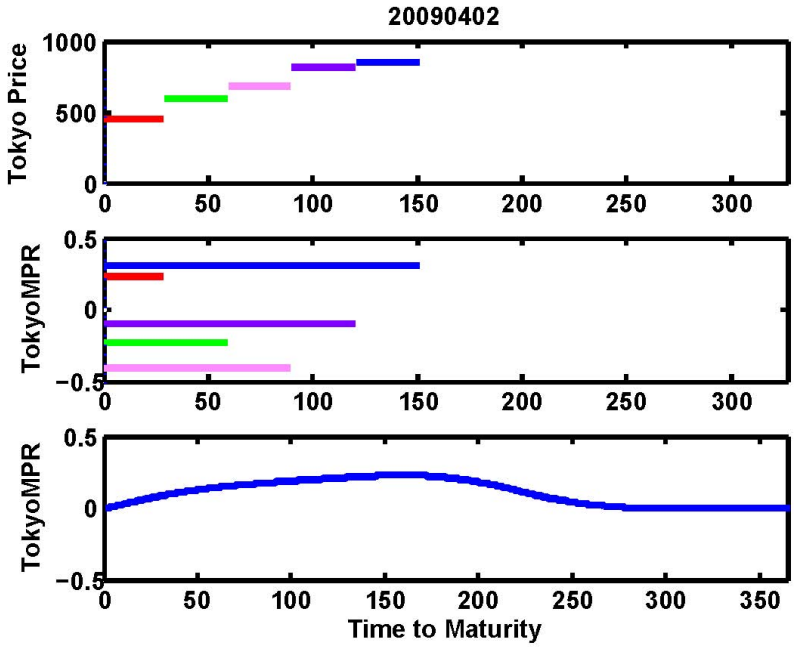

Figure 12: Tokyo Future Prices and MPR on 20090402

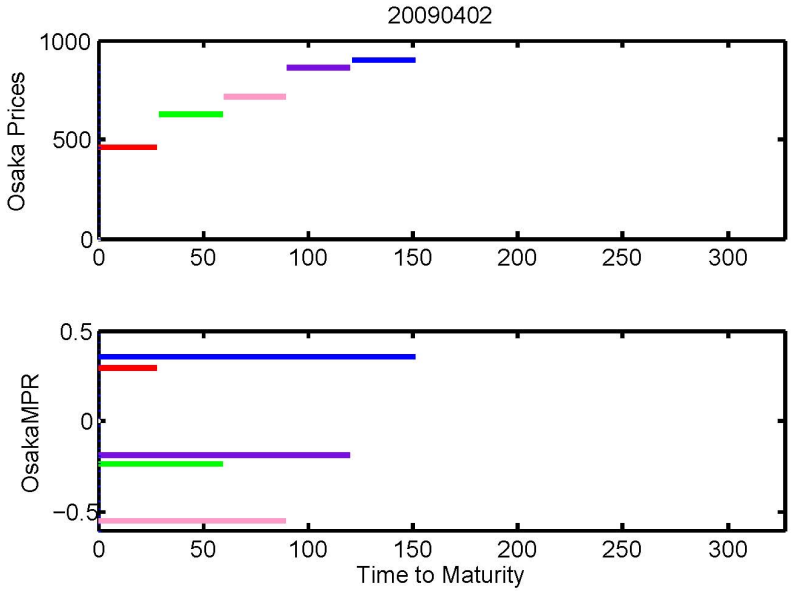

Figure 13: Osaka Future Prices and MPR on 20090402

4.2.2 Time Dependent MPR for contracts per trading day

Previously, we have assumed that no matter how long the time to maturity is, the contract of 1 specific type has the same MPR. While this assumption has clearly shown the property of Osaka Index; Tokyo has a different characteristic that MPR varies with different time to maturity. Thus, we derive a general form of $\hat{\theta}_t^i$ for each i contract per trading day, $i = 1, 2, 3, ...12$ as:

$$\begin{aligned}\arg\min_{\hat{\gamma}_k} \sum_{i=1}^{12} = \Bigg(& F_{CAT(t,\tau_1^i,\tau_2^i)} \\ & - \Big(\int_{\tau_1^i}^{\tau_2^i} \hat{\Lambda}_u du - \hat{a}_{t,\tau_1^i,\tau_2^i} \hat{X}_t \\ & - \int_t^{\tau_1^i} \sum_{k=1}^{K} \hat{\gamma}_k \hat{h}_k(u_i) \hat{\sigma}_{u_i} \hat{a}_{t,\tau_1,\tau_2} e_p du_i \\ & - \int_{\tau_1^i}^{\tau_2^i} \sum_{k=1}^{K} \hat{\gamma}_k \hat{h}_k(u_i) \hat{\sigma}_{u_i} e_1^\top A^{-1} [exp\{A(\tau_2^i - u_i)\} - I_p] e_p du_i \Big) \Bigg)^2 \end{aligned} \tag{29}$$

where $h_\kappa(u_i)$ is a vector of spline basis,$\gamma_(\kappa)$ defines coefficients. Empirically, on date 20090402, 5 contracts are being traded, thus we have $i = 1, 2, 3, 4, 5$,and the MPR of the Pacific Rim Index contracts traded on this day is calibrated using cubic polynomios with numbers of knots equal to 5. The lower panel of Figure 12 has shown the time dependent MPR of Tokyo's contracts. We see the same trend as its constant MPR, that when time to maturity equals to 120, which represents the contracts M, the MPR reaches to its peak. This has also reflected seasonal variance's influence, as in July, seasonal variance of Tokyo has the highest value.

4.3 Prices with Implied MPR

With the MPR implied from 2 parametrization methods: constant MPR and spline MPR, we could proceed with estimating the prices with equation. Table 5.1 has shown the estimated prices with MPR from different parametrization methods.

Pacific Rim Index future prices with constant MPR per contract per trading day, shown in column 4, have fully replicated the prices from Bloomberg, in terms that the methods applied is just an inversion of equation 21. The future prices with time variant MPR has shown the influences from the MPR. When MPR is high for June and July, the prices calculated with spline MPR is higher than its estimate with constant MPR. Further, we also calculated the prices by assuming MPR equals to zero, through which we see that when MPR is bigger than 0 for contracts J9 and Q9, shown in Figure 11, the prices with zero MPR is smaller; when MPR is negative with contracts K9, M9 and N9, the prices with zero MPR is bigger.

Tokyo	$F_{CATBloomberg}$	$F_{CAT,\hat{\theta}_t^0}$	$F_{CAT,\hat{\theta}_t^i}$	$F_{CAT,\hat{\theta}_t^{spl}}$
J9	450.00	409.15	450.00	417.66
K9	592.00	630.69	592.00	651.38
M9	682.00	740.10	682.00	785.36
N9	818.00	832.60	818.00	858.90
Q9	855.00	815.40	855.00	832.79
Osaka	$F_{CATBloomberg}$	$F_{CAT,\hat{\theta}_t^0}$	$F_{CAT,\hat{\theta}_t^i}$	$F_{CAT,\hat{\theta}_t^{spl}}$
J9	460.00	410.31	460.00	–
K9	627.00	662.84	627.00	–
M9	716.00	783.85	716.00	–
N9	861.00	882.46	861.00	–
Q9	899.00	860.24	899.00	–

Table 3.1 Tokyo & Osaka future prices estimates on 20090402 from different MPR parametrization methods

4.4 Risk Premium with respect to zero MPR

Finally, we relate the market price of risk $\hat{\theta}_t^i$ to the Risk Premium (RP), which is defined as:

$$RP = F_{CAT,\hat{\theta}_t^i} - F_{CAT,\hat{\theta}_t^0} \tag{30}$$

by which, we tried to capture the power of market price of risk. Figure 14 and Figure 15 shows the the future prices of Tokyo and Osaka contract Q9, as well as the corresponding MPR and Risk Premium under different parametrization methods.

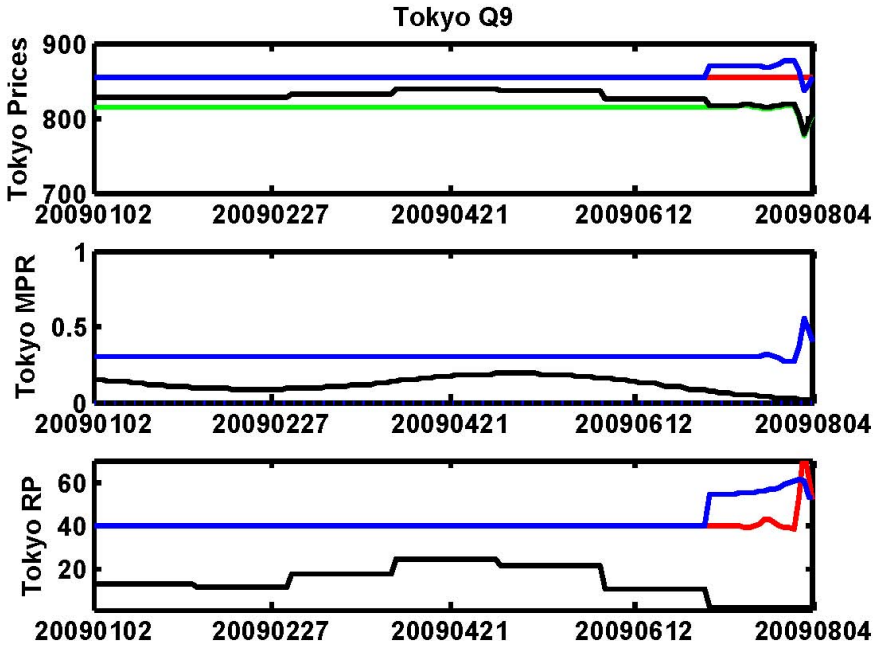

Figure 14: Prices(upper), MPR (middle)and Risk Premium(down) of Tokyo Futures traded between 20090102- 20090804.

Red solid line denotes the prices from Bloomberg, blue solid line is the results from constant MPR, and Black solid line is from time variant MPR. They are all compared with the green line, denoting the prices calculated with MPR equals to zero. As Osaka cannot be applied to time variant MPR methods, we could not have black solid line which denotes price with spline MPR in Figure 15.

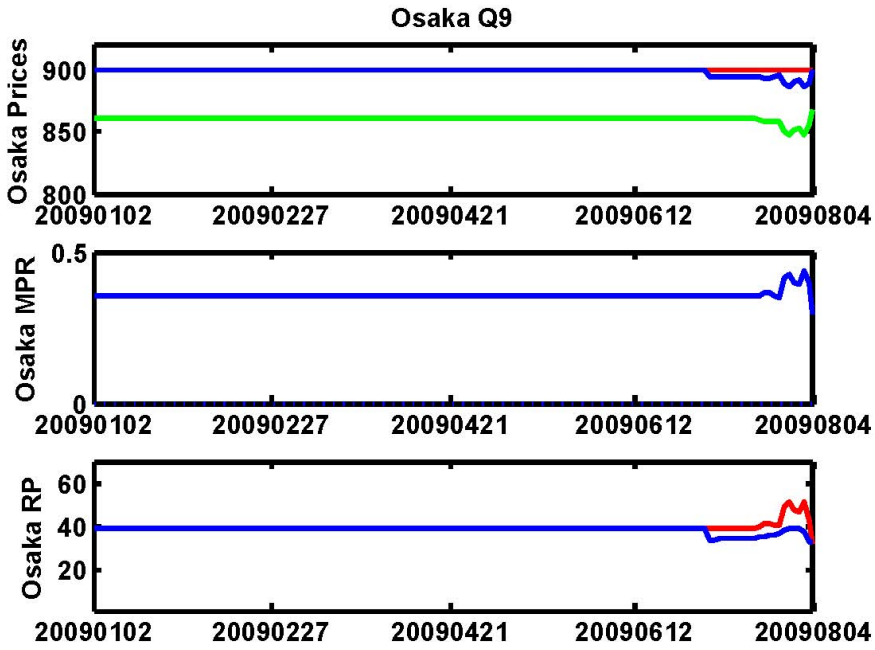

Figure 15: Prices(upper), MPR (middle)and Risk Premier(down) of Osaka Futures traded between 20090102- 20090804.

From the results of Q9 of both Tokyo and Osaka, we observe constant behavior of prices and MPR before July, the associated Risk Premier has also shown a constant property. However, deviation happens when approaching to the measurement period, except for the results calculated from Spline MPR.

5 Conclusion

In this study, we analyze the temperature dynamics in 4 Asian cities, Tokyo, Osaka, Taipei and Beijing by a higher order continuous-time autoregressive model. As Tokyo and Osaka's temperature are being traded on Chicago Mercantile Exchange, we analyze the future prices of these two cities' temperature index by applying the stochastic pricing model.As temperature is an non-tradable asset,we introduced the concept of market price of risk in order to deal with the iliquidity and incompleteness of the temperature market. We implied the market price of risk in two different parametrization methods: firstly as a piecewise constant linear function, further as time variant for all the contracts with different time to maturity. It is by these methods we have not only achieved a complete replication of the real prices on CME, but also detected the influences of the seasonal variance on the market price of risk. We further studied the risk premier with respect to the case when market price of risk equals to zero. It is trough this process we further justified that the market price of risk is not zero, it has a seasonal structure coming from the seasonal variance in temperature dynamics, and it plays an important role in driving the estimated prices' deviation from the future spot market, especially when approaching maturity.

References

Alaton, P., Djehiche, B. and Stillberger, D. (2002). On modelling and pricing weather derivatives, *Appl. Math. Finance* 9(1): 1-20.

Barrieu, P. and El Karoui, N. (2002). Optimal design of weather derivatives, *ALGO Research* 5(1).

Benth, F. (2003). On arbitrage-free pricing of weather derivatives based on fractional brownian motion., *Appl. Math. Finance* 10(4): 303-324.

Benth, F., Koekebakker, S. and Saltyte Benth, J. (2007). Putting a price on temperature., *Scandinavian Journal of Statistics* 2007 .

Benth, F. and Saltyte Benth, J. (2005). Stochastic modelling of temperature variations with a view towards weather derivatives., *Appl. Math. Finance* 12(1): 53-85.

Brody, D., Syroka, J. and Zervos, M. (2002). Dynamical pricing of weather derivatives, *Quantit. Finance* 3: 189-198.

Campbell, S. and Diebold, F. (2005). Weather forecasting for weather derivatives, *American Stat. Assoc.* 100(469): 6-16.

Cao, M. andWei, J. (2004). Weather derivatives valuation and market price of weather risk, *The Journal of Future Markets* 24(11): 1065- 1089.

Davis, M. (2001). Pricing weather derivatives by marginal value, *Quantit. Finance* 1: 305-308.

Dornier, F. and Querel, M. (2000). Caution to the wind, *Energy Power Risk Management,Weather Risk Special Report* pp. 30-32.

Hädle, W. and López, B.(2009). Implied Market Price of Weather Risk, 1-39.

Hamisultane, H. (2007). Extracting information from the market to price the

weather derivatives, *ICFAI Journal of Derivatives Markets* 4(1): 17-46.

Hung-Hsi, H., Yung-Ming, S. and Pei-Syun, L. (2008). HDD and cDD option pricing with market price of weather risk for taiwan, *The Journal of Future Markets* 28(8): 790-814.

Jewson, S., Brix, A. and Ziehmann, C. (2005). *Weather Derivative valuation: The Meteorological, Statistical, Financial and Mathematical Foundations.*, Cambridge University Press.

Karatzas, I. and Shreve, S. (2001). *Methods of Mathematical Finance.*, Springer Verlag, New York.

Mraoua, M. and Bari, D. (2007). Temperature stochastic modelling and weather derivatives pricing: empirical study with moroccan data., *Afrika Statistika* 2(1): 22-43.

Platen, E. and West, J. (2005). A fair pricing approach to weather derivatives, *Asian-Pacific Financial Markets* 11(1): 23-53.

PriceCooperWaterhouse(2005) Weather Derivatives *Weather Risk Management Association.*

Richards, T., Manfredo, M. and Sanders, D. (2004). Pricing weather derivatives, *American Journal of Agricultural Economics* 86(4): 1005-1017.

Declaration of Authorship

I hereby confirm that the thesis I am submitting is entirely my own original work except where otherwise indicated. I am aware of the University's regulations concerning plagiarism, including those regulations concerning disciplinary actions that may result from plagiarism. Any use of the works of any other author, in any form, is properly acknowledged at their point of use.

Students signature:

Name (in Capitals) : Yue Jiao

Date of Submission : September 15, 2009